The Effects of Variable Quadriceps and Hamstring Loading Configurations on Knee Joint Kinematics During *In Vitro* Testing

By

Sami Shalhoub

Submitted to the graduate degree program in Bioengineering and the Graduate Faculty of the University of Kansas in partial fulfillment of the requirements for the degree of Master of Science.

_____

Chairperson Dr. Lorin Maletsky

_____

Dr. Sara Wilson

_____

Dr. Terry Faddis

Date Defended: June 5, 2012

The Thesis Committee for Sami Shalhoub

certifies that this is the approved version of the following thesis:

The Effects of Variable Quadriceps and Hamstring Loading Configurations on Knee Joint Kinematics During *In Vitro* Testing

_____

Chairperson Dr. Lorin Maletsky

Date approved: June 6 2012

## Abstract:

Previous studies have highlighted the importance of the hamstrings and quadriceps muscles on knee joint mechanics and the effects of their pathologies. It is crucial that the resultant force of theses musculature be accurately represented in *in vitro* simulation. This study has two objectives to be examined during a deep knee squat: 1) measure the patellofemoral kinematics as a function of different loading configurations of the extensor mechanism and 2) measure the changes in tibiofemoral kinematics after including a direct hamstrings load. Fourteen fresh frozen cadavers were tested using a custom designed muscle loading rig. The rig can statically load the individual heads of the quadriceps and the hamstrings in their anatomical orientation using dead weights or directly drive the rectus femoris quadriceps muscle using a stepper motor.

Patellofemoral flexion and shift were the only kinematics that changed significantly between the single line and the physiological based distributed loading configuration of the extensor mechanism, with the largest difference of 2.8° and 0.9 mm at 15° and 45° knee flexion respectively. A weak vastus medialis induced an average lateral shift of 1.5 mm and an external rotation of 0.8° while a 0.9 mm medial shift and 0.6° internal rotation was seen when simulating a weak vastus lateralis relative to the physiological based distributed configuration. The change in patellofemoral kinematics was caused by the non-parallel forces to the axis of the femur generated from the VM and the VL. The flexion moment generated from these forces in the sagittal plane decreased patellar flexion. The vastus lateralis load was larger than that of the vastus medialis causing the resultant force in the frontal plane to be more externally rotated.

When the hamstrings were loaded throughout the flexion cycle the femoral lateral condyle lowest point was more anterior with the largest difference of 1.1 mm at 80° knee flexion. For the medial femoral condyle lowest point, loading the hamstrings shifted the lowest point 0.9 mm

posterior until 40° flexion. At this flexion angle, the medial lowest point became more anterior for the rest of the flexion cycle (0.9 mm on average). The hamstrings also decreased the medial and lateral lowest point range of motion by 1.7 mm and 0.9 mm respectively. The change in tibia femoral kinematics was larger in deeper knee flexion when the hamstrings were loaded which is due to the increase in the hamstrings moment arm, but it is unclear at this point whether the reduction in tibial internal rotation is due to the isometric loading configuration of the hamstrings.

The results from this study demonstrated that different muscle loading configurations of the extensor mechanism and muscle weakness significantly influence patellofemoral shift and tilt while increasing the co-contraction between the quadriceps and hamstrings significantly reduces tibial anterior translation and internal rotation. The study has aided in describing the effects of different muscle loading configurations on knee joint kinematics from simulations and provided important experimental data to investigate changes to improve dynamic simulations using the Kansas Knee Simulator.

## Acknowledgements

This thesis would not have been possible without the guidance and the assistance of several individuals who have helped me thorough my graduate study at KU and I owe a special thanks to them.

- First and foremost to my family: my mom, dad and sister for their support, encouragement and believing in me even when I didn't believe in myself. Without their love and support none of this would have been possible.

- To my advisor, Dr. Lorin Maletsky for giving me the opportunity to be part of his lab, challenging and guiding to be the best researcher I can be. I have learned a lot from him as a researcher and a person.

- To Dr. Wilson, and Dr.Faddis and all the faculty members and staff of the Bioengineering program and Mechanical engineering departments for their time and effort.

- To past and current members of the Experimental Joint Biomechanics Research Laboratory : Fallon Fitzwater, Adam Cyr, Kaity Fucinaro, Mark Komosa, Lauren Ferris, Amit Mane, and Amber Reeve for spending many hours and late nights working in the lab , engaging in my pointless discussions, tolerating my singing and making my day at lab more entertaining with their amazing sense of humor.

- Charles Gabel and Ash Shadrick for their advice and patience in the machine shop and for helping me build and design the MLR.

## List of abbreviations

**BF** Biceps femoris

**BFH** High BF load II

**BFL** High BF load I

**KKS** Kansas Knee Simulator

**Ma** Manual manipulation

**MLR** Muscle Loading Rig

**Mo** Motor manipulation

**MR** Magnetic resonance

**NMa** Normal manual manipulation

**NMO** Normal motor manipulation

**PF** Patellofemoral

**QH** Quadriceps and hamstrings

**QO** Quadriceps only

**RF** Rectus femoris

**SM** Semimembranosus

**SMa** Single line manual manipulation

**SMH** High SM load I

**SML** High SM load II

**SMO** Single line motor manipulation

**ST** Semitendinosus

**TF** Tibiofemoral

**VI** Vastus intermedius

**VL** Vastus lateralis

**VM** Vastus medialis

**WVL** Weak vastus lateralis

**WVM** Weak vastus medialis

## List of Figures:

## List of Tables:

# Table of Contents:

## 1. Introduction

The knee's anatomical geometry, muscle loading condition, and it six degree of freedom makes it one of the most complex joints in the human body. The hamstrings and the quadriceps musculature loading condition such as, loading vector direction, co-contraction ratio, and activation levels, play a large role in joint stabilization and locomotion during daily living activities. These factors make it difficult to simulate physiological kinematics and kinetics during cadaveric studies. Pathologies that affect these musculatures cause abnormal loading conditions and kinematics that often result in pain and loss of movement to this joint. The ability to replicate the loading condition of the knee during in vitro testing is essential to replicate the knee physiological kinematics and kinetics and investigate the effects of quadriceps and hamstring pathologies on the knee joint.

The Kansas Knee Simulator (KKS) [1] along with other knee simulator have been used to replicate the physiological conditions of activities of daily living on cadaveric specimens. The ability and accuracy of these simulators to replicate the physiological knee condition has been debated, since they do not include hamstrings load, and they do no simulate the individual heads of the quadriceps. Quantifying the effects of different quadriceps and hamstrings loading configurations on knee joint kinematics will aid in better understanding of the results from these simulations. The results will also suggest modifications to these simulators, if needed, to improve their ability to replicate physiological conditions.

The current research had two main objectives; 1) measure in vitro the change in patellofemoral tracking measures due to different loading configuration of the extensor mechanism, and 2) examine and calculate the variation in tibiofemoral kinematics cause by a

direct hamstring load. The results of this study will give a better understanding of the effects of different muscle loading configuration on knee joint kinematics and can introduce parameters that will aid in creating *in vitro* simulation that better represent *in vivo* data.

Literature review of the quadriceps and hamstrings anatomy and physiology along with their pathologies and their effect on knee joint kinematics are described in Chapter 2 of this report. The literature review also includes a description of current knee joint *in vitro* testing methods and their limitations. Chapter 3 explains the methodology developed to achieve the first two objectives and the results of varying the quadriceps loading configurations on patellofemoral kinematics. Chapter 4 details the effects of the inclusion of hamstrings load on tibiofemoral lowest point and internal external rotation during dynamic simulations. The last chapter contains an overall summary and evaluation of the research, future works that need to be completed, and how the results can be used in the future.

# 2. Literature Review

This literature review focuses on muscle anatomy and physiology related to the knee joint as well as exploring methods and parameters used in current and past *in vitro* tests. The review in this chapter covers the primary and secondary muscles of the lower limb responsible for knee joint motion, summarizing their anatomical structures and attachment sites, as well as their specific contribution to the overall motion. The chapter also includes a summary of methods and parameters of previous and current *in vitro* studies, describing their advantages and disadvantages and how the limitation of these parameters could have affected the outcomes of these studies.

## 2.1. Muscles Affecting the Knee Joint

The muscles of the thigh and the leg contain the two main muscle groups that affect the knee joint. The muscles of the thigh are divided into three main muscle groups: anterior, medial and posterior [2, 3] (Figure 2.1). The anterior and posterior muscles consisting of the quadriceps and the hamstrings are considered to be the primary flexor and extensor mechanism of the knee joint and will be described in detail in later sections of this chapter (Sec 2.2 & 2.3). The only muscle that affects knee joint kinematics from the medial thigh muscle group, also known as the adductor muscles, is the gracilis. The gracilis originate from the lower part of the symphysis pubis and pubic arch and inserts onto the medial surface of the proximal tibia [3, 4]. In addition to adducting the femur, the gracilis medially rotates the tibia relative to the femur [3, 4].

The leg muscles include three different muscles that affect knee kinematics; popliteus, plantaris and gastrocnemius (Figure 2.2). Because of the location of the origin near the lateral collateral ligament and insertion into the posterior surface of the tibia near the oblique line, the

popliteus plays a role in flexion and rotation of the femur relative to the tiba [3-5] (Figure 2.2 A). The gastrocnemius originates from both the medial and lateral femoral condyles and inserts onto the calcaneus while the plantaris only originates from the lateral condyle and inserts beside the insertion site of the gastrocnemius [4] (Figure 2.2 B, C). Both the gastrocnemius and the plantaris assist in knee flexion, although the actions of the plantaris are often minimal [4].

## 2.2. Quadriceps Muscles

### 2.2.1. Quadriceps Anatomy and Physiology

The quadriceps is one of the largest muscle groups in the human body. In addition to being the main active stabilizer for the PF joint, the quadriceps serve as the primary knee extensor mechanism during walking, running, and other activities of daily living [6]. There are four individual muscles that make up the quadriceps which includes the rectus femoris (RF), vastus intermedius (VI), vastus lateralis (VL), and vastus medialis (VM). The VM and the VL have distinguishable longus and oblique parts (Figure 2.3) [7-10]. The individual heads of the quadriceps insert onto the entire proximal surface of the patella, spreading along the medial and lateral edge through a shared multi-laminar tendon most commonly described in the literature as a three layer arrangement, consisting of a superficial, intermediate, and deep layer [7, 8, 10]. The superficial layer consists of the RF which runs parallel to the shaft of the femur and inserts onto the superior anterior portion of the patella [3, 8]. Some of the superficial fibers of the RF run over the patella and join the patellar ligament [8, 10-12].

The VL, the largest component of the quadriceps, and the VM makes up the intermedius layer of the quadriceps [8, 10]. The VL and the VM run along the lateral and medial side of the RF and insert onto the superior part of the patella with a 35° and 45° angles respectively off the anatomical axis of the femur in the frontal plane (Figure 2.3)[8, 13]. The VL inserts onto the

superiolateral edge of the patella [8, 10, 11, 14]. Some of the lateral fibers of the VL that cross the patella become a part of the lateral patellar retinaculum [11, 14]. The VM inserts on the opposite side of the patella, more specifically the superiomedial edge of the patella [8, 10, 11, 14]. The distal fibers of the VM that extend beyond the patella help form the medial patellar retinaculum [11, 14].

The most distal portion of the VM and the VL are often referred to in literature as the vastus medialis oblique and vastus lateralis oblique respectively [8, 14-17]. The VM inserts onto the patella with 50°± 5° posterior angle relative to the long axis of the femur, while the VL inserts with 45°± 5° posterior angle (Figure 2.3)[8, 13]. Both the VM and the VL are believed to be the major contributors to patellar mediolateral stability by applying more direct medial and lateral forces respectively [10, 18]. Also, since the VM and VL do not run parallel to the axis of the femur in the sagittal plane, they exert posterior forces on the patella generating a compressive force that maintains the patella in the trochlear groove[8, 13].

The VI, also known as the deep layer of the quadriceps, originates from the lateral intermuscular septum and shares a common origin with the VM and VL [3, 4]. The VI runs parallel to the RF and inserts posterior to the VM and VL insertion site on the patella [3, 8, 10]. Some literature suggests that the superficial tendon of the VI joins the RF to create the suprapatellar tendon [10].

### 2.2.2. Quadriceps Pathologies

Pathologies of the quadriceps greatly affect one's ability to perform activities of daily living since the quadriceps is the primary extensor mechanism of the knee joint [6]. Quadriceps tendon rupture is a major injury that occurs more frequently in older patients. it is easy to diagnose with

symptoms like a loss of active knee extension, knee pain, and suprapatellar depression [19, 20]. Different surgical techniques exist to repair the ruptured tendon and restore the quadriceps functionality with high success rates reported in the literature [21-24].

PF disorders such as PF joint pain and instability (dislocation and maltracking) have been primarily attributed to weakness in the quadriceps, more specifically weakness in the VM [25-27]. PF joint pain is described as pain in the anterior region of the knee [25, 26], while patellar instability is referred to as abnormal patellar tracking of the patella in the trochlear groove during daily activities [28]. Both disorders affect young and adult patients, with a higher occurrence in women and physically active individuals [29, 30]. The above disorders occur when the VM is weakened and the lateral force applied on the patella through the VL displaces the patella laterally. Weakness in the VM often occurred after patella dislocation or after an invasive surgery like total knee replacement. Senavongse *et al.* and Farhamand *et al.* have shown that weakness of the VM can shift the resultant force of the quadriceps up to 6° laterally in the frontal plane and decrease the force needed to translate the patella 5 mm laterally by 20 N [31, 32]. Weakness and injuries of the VM can be treated noninvasively through a series of exercises that restore its strength [33]. Other noninvasive methods include patellar taping which activates the VM at an earlier time than the VL and optimizes the interaction location between the patella and the trochlear groove [34, 35]. In addition to the noninvasive methods, some surgical techniques exist to repair the VM including reattaching the VM to ligaments of the medial retinaculum [36], or by lateral release of the VL tendon or the lateral retinaculum [37, 38]. Both methods have reportedly been successfully at restoring the VM functionality to restrain patellar lateral translation [36-38].

## 2.3. Hamstrings Muscles Anatomy

### 2.3.1. Hamstrings Anatomy and Physiology

The posterior muscle of the thigh, also known as the hamstrings, consists of three individual muscles: the semimembranosus (SM), semitendinosus (ST), and the biceps femoris (BF) (Figure 2.1 &Figure 2.4) [2-4]. Gray and Hartwig described the anatomy and physiology of each individual head of the hamstrings in their respective books [3, 4]. The SM originates from the superior portion of the ischium tuberosity and inserts into the superiomedial part of the tibial shaft near the insertion of the popliteus muscle. The second muscle of the hamstrings, the ST, originates just below and medial to the origin site of the SM on the ischium tuberosity. The ST crosses over the tibial collateral ligaments and inserts on the most medial surface of the tibial plateau. Both the SM and the ST form what is known as the medial hamstrings. The BF is considered to be the lateral portion of the hamstrings and has two heads, a long head that shares the same origin with the ST, and a short head that originate for the proximal shaft of the femur between the adductor magnus and the VL [39]. Both the short and long heads merge together but later split into two insertion sites that cover the head of the fibula[3, 4, 39]. found Wickiewicz *et al.* found a 3:2 ratio of the cross sectional area between the lateral and medial portions of the hamstrings [40].

The hamstrings are mainly responsible for flexing the knee joint and extending the hip joint. When the foot is planted on the ground the hamstrings extends the hip and aids in translating the trunk forward. During activities where the truck is not translating, like sitting or squatting, the hamstrings flex the foot towards the trunk. During walking, the hamstrings activate prior to foot strike to decelerate the knee motion and assist in extension of the hip joint shortly after foot strike. In addition to being the main flexor muscle of the knee, the hamstrings play a

big role in tibial internal/external rotation after 20° flexion. The BF is able to rotate the tibia externally with its lateral insertion site, while the ST and the SM rotate the tibia internally with their medial attachments sites.

### 2.3.2. Hamstrings Pathologies

The hamstrings is the most commonly injured muscle group in the body with the most common injuries being hamstrings tear and strain [41-43]. Garrett *et al.* and Kujala *et al.* suggested that hamstrings tear usually occur during eccentric contraction [44, 45]. Of the hamstrings tear and strain injuries, 53% involve the BF compared to 47% involving the SM and ST combined [46]. These injuries typically happen at the muscle tendon junction, although it is not uncommon for the injury to occur in other places along the muscle itself [47]. Different technologies exist to diagnose hamstrings tears including magnetic resonance imaging and ultrasounds as well as feedback from clinical evaluation [47-49]. Treatment for these injuries can vary depending on the severity. Treatments can range from clinical rehabilitation to surgical repair if the tendon was completely ruptured [43, 44, 47]. A study by Proske *et al.* have found that even though hamstrings rehabilitation is usually successful, people with a previous history of these injuries are more prone to reinjure their hamstrings [50].

These injuries, along with invasive surgeries such as ACL reconstruction that utilizes hamstrings autografts and total knee replacement, can cause muscle weakness in the hamstrings which can have major effects on the knee joint. Weakness of the hamstrings in the intact knee causes added stress and strain in the surrounding muscle and soft tissue of the joint to compensate for this deficiency. This is especially seen in the ACL and multiple studies have reported an increase in ACL strain when the hamstrings loading was not present [51-53]. It has also been reported that there is a decreased tibial internal rotation and femoral anterior translation

when the hamstrings are unloaded [53-55]. After ACL reconstruction, studies have shown that deficiencies in hamstrings strength could decrease knee stability and increase knee laxity as well as the ability to rotate the tibia [56, 57]. In addition, reduction in the strength of the hamstrings post total knee replacement could lead to later post cam engagement that could cause dislocation of the knee joint.

### 2.4. Current *In Vitro* Testing Methods and Limitations

Cadaveric studies are used to increase knowledge of the human body and develop and improve treatments for different pathologies.

*In vitro* knee testing has been used to understand the knee joint kinematics [58, 59], different surgery techniques [56, 60], and improvement of orthopedic joint replacements [61, 62]. Cadaveric knee testing can be categorized by the loading conditions as passive (unloaded) studies and loaded studies. Passive studies are usually used to determine the range of motion of knee kinematic and the contribution of soft tissue [58, 63-65]. Loaded *in vitro* research utilizes dynamic simulators and/or load frames to study the effects of muscle loading and muscle pathologies on kinematics [18, 27, 59, 66]. Using dynamic simulators, researchers are able to replicate and study the kinematics and loading patterns of different activities of daily living like walking or squatting, and investigate the effect of different testing parameters such as load condition or implantation of prosthetic geometries [53, 67, 68].

Early knee joint cadaveric testing was performed on simple and static loading rigs [58, 69]. Dynamic motion was achieved by the researcher manually manipulating the knee. As technology advanced and improvement were made in the field of robotics, more complex motor or hydraulic control rigs [1, 13, 53] and 6 degree of freedom robots [52, 70, 71] were built to examine knee

joint mechanics and kinetics. To achieve useful clinical results, it is necessary for these rigs to replicate the *in vivo* loading condition of the knee.

Although cadaveric testing provides insight into the behavior of the knee joint, there are multiple limitations to these types of studies. The age of specimens is generally limited to an older age group and is not necessarily representative of the entire population. In addition, passive studies have reported sensitivity to rig design, orientation of the specimen, and research variability [58, 63, 65, 72]. Dynamic simulations rely highly on loading configuration parameters such as specimen orientation, muscle loading magnitude and directions [55].

McWilliams *et al.* [53] loaded both the medial and lateral hamstrings statically, and this loading condition is common in many hamstrings studies [52, 66], assuming that both heads of the hamstrings contract similarly and do not vary in load throughout the flexion cycle. This is an inaccurate representation of *in vivo* hamstrings loadings which could have a significant affect on kinematics. A common practice during *in vitro* studies is determining muscle loading contributions based on their cross sectional area [13, 53, 55, 59], which make the assumption that the ratio of these load is constant throughout the cycle and does not take into consideration the different activation time of each individual muscle. In addition, a small number of literature currently exist that relates the ratio of quadriceps to hamstrings load throughout the flexion making it hard to dynamically load these muscle to preform physiological simulation.

Another challenge of *in vitro* testing is data acquisition at a static flexion position of the knee [13, 32, 73]. The kinematics obtained from these studies include limited measurements taken at discrete points in the flexion cycle and do not provide information about dynamic kinematics. It

also does not provide insight into the difference between the flexion and extension cycle that has been reported in previous studies.

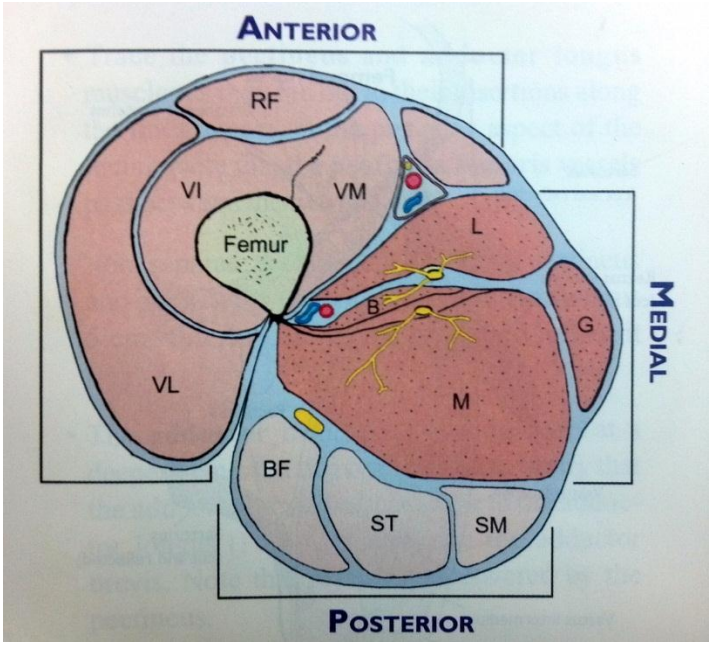


**Figure 2.1: Transverse section of a right thigh including the 3 muscle groups of the thigh anterior, medial, posterior. B adductor pervis, G gracilis, L adductor longus, M adductor mangus, BF biceps femoris, SM semimembranosus, ST semitendinosus, RF rectus femoris VI vastus intremedius, VL vastus lateralis, VM vastus mediali [2].**

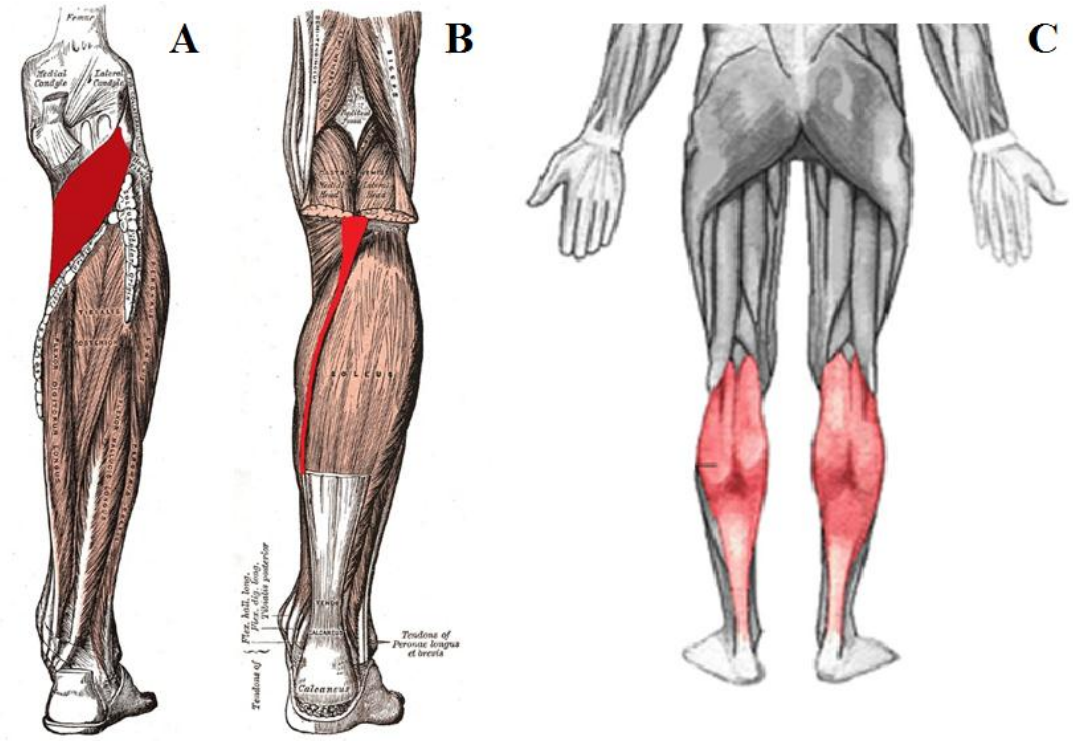


**Figure 2.2: Origin and insertion site of the leg muscles that effects knee joint motion with the shaded muscle representing (A) popliteus, (B) plantaris, and (C) gastrocnemius [3].**

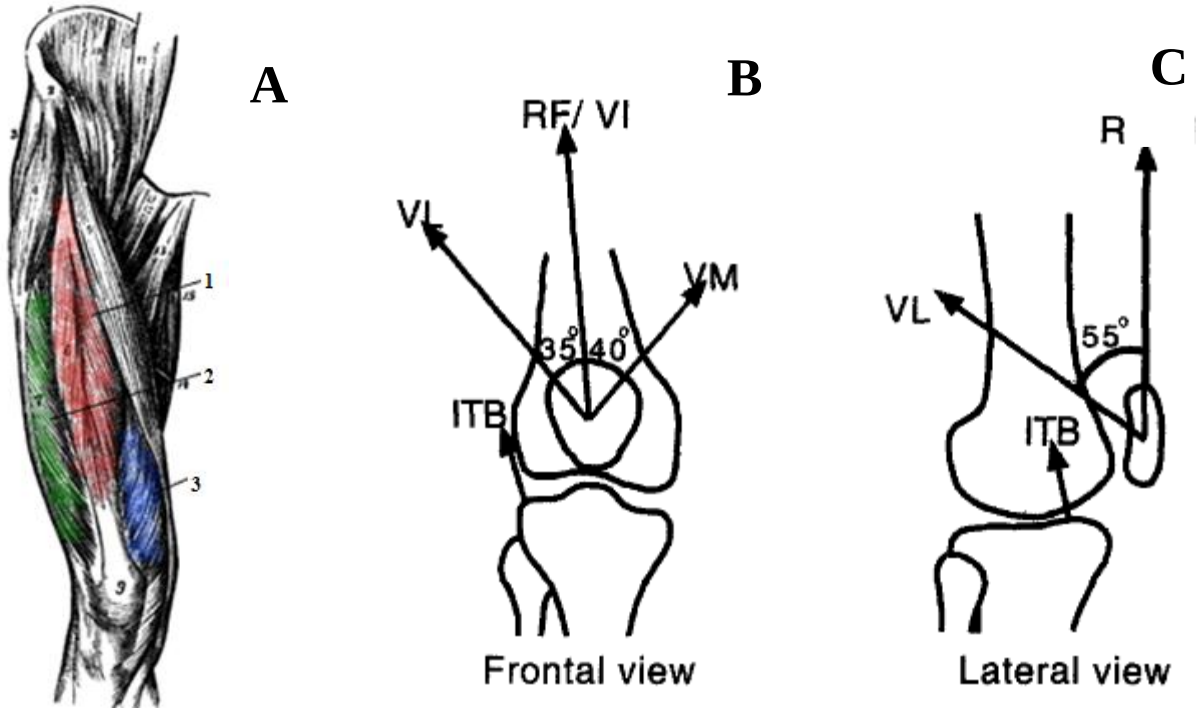


**Figure 2.3: Image of right leg showing (A) Anatomy of the quadriceps with the individual heads highlighted; vastus lateralis (green), rectus femoris and vastus intermedius (red), and vastus medialis (blue) [3] and the orientation of theses head (B) frontal plane and (C) sagittal plane[55].**

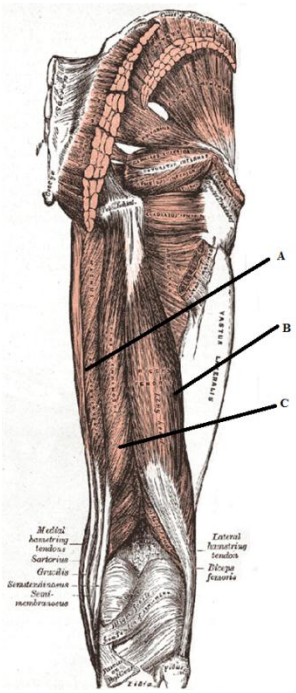


**Figure 2.4: Image of right leg showing the anatomy of the individual heads of the hamstrings; (A) semimembranosus, (B) biceps femoris and (C) semitendinosus[3].**

# 3. Variation in Patellofemoral Kinematics due to Different Quadriceps Loading Conditions

## 3.1. Introduction

The quadriceps is the sole muscle group that crosses the PF joint, making it the primary contributor of the knee extensor mechanism. PF joint disorders such as lateral patellar compression syndrome, anterior knee pain, and recurrent subluxation, or dislocation occurs frequently in the general population and have a substantial effect on one's ability to perform activities like walking, climbing, kneeling, and other activities of daily living [25, 26, 74]. Multiple factors contribute to PF joint disorders, with the leading cause being muscle weakness of the quadriceps, specifically the VM [26, 37, 59, 75]. Identifying the variation in PF kinematics due to changes in the loading configurations of the individual heads of the quadriceps could assist in determining PF disorders and suggest some treatment methods based on muscle strengthening.

*In vitro* testing is one of the alternative methods to *in vivo* testing to measure PF kinematics [59], contact area [13], and the effect of muscle weakness on the knee [27, 38]. Being able to replicate *in vivo* kinematics and loading conditions during cadaveric testing is crucial to obtaining meaningful PF kinematics that can be related to clinical findings for both normal and pathological conditions. To create accurate physiological loading one must consider the line of action of each muscle, the percent contribution of these muscles, and the total force that needs to be applied during simulation. Many dynamic knee simulators are quadriceps driven and only load RF and VI parallel to the axis of the femur [1, 53, 76]. The single line of action loading condition using the RF and VI of these simulators makes the assumptions that: 1) the resultant force of the quadriceps is in the direction of the RF and VI fiber orientation and 2) the quadriceps

only produce a force that is not parallel to the long axis of the femur. The exclusion of the other heads of the quadriceps could greatly affect PF kinematics because the VM and the VL insert into the superomedial and superolateral edges of the patella respectively, creating a sheet that surround and stabilize the patella in the femoral groove [8]. In addition, the VM and the VL fibers in the sagittal plane have a posterior slope relative to the femur which, when loaded, creates a force that drives the patella into contact with the femoral groove [8, 40]. The exclusion of these loads, that are not along the axis of the femur, in the single line of action simulation decreases patella stability and could lead to changes in the PF kinematics, especially patellar tilt, glide, and flexion.

Due to the complexity of the extensor mechanism, Researchers have been interested in determining if it could be simulated with a single line of action muscle load and whether the conclusions drawn from these types of simulations can be correlated to clinical findings. Therefore, the three main goals to this study. First, to compare the PF kinematics using a single line of action quadriceps load (loading the RF and VI only) with that of a more physiologically based distributed loading (loading individual heads of the quadriceps in their anatomical orientation). Second measure the effect of limited medial and lateral vasti loading during dynamic knee simulations, and finally to examine the effects VM and VL weakness on PF kinematics. It was hypothesized that PF kinematics would differ greatly with application of more physiological loading conditions compared to the single line of action loading and have a decreased range of patellar motion during the entire flexion cycle. The second hypothesis of this study is related to altering the percent of the total load on the individual heads of the quadriceps. The hypothesis was that weak VM or VL would vary PF kinematics compare to the normal configuration. The variation will be seen especially in patellar glide where weak VM will

translate the patella laterally while a weak VL will cause the patellar to shift medially. Investigation of different loading conditions and their limitations would aid in the creation of simulations that better replicate both normal and pathological cases while identifying the contribution of the individual heads of the quadriceps to the kinematics would aid in understanding the effect of muscle weakness on PF pathologies.

## 3.2. Materials and Methods

### 3.2.1. Muscle Loading Rig

A custom Muscle Loading Rig (MLR) was developed by the author to load the muscle groups of the hamstrings and the quadriceps individually in their anatomical directions. The MLR consists of a mounting frame for the knee, steel plates with eye bolts and pulleys that provide attachment sites to direct each head of the quadriceps and the hamstrings muscles in their physiological orientation (Figure 3.1). The steel plates and pulleys can be adjusted to change the orientation of the muscle line of action and redirect the load being applied to the muscles in the correct physiological direction. The knee can be moved through its flexion range either manually or through a motor attached to the RF and the VI. Muscle loading was accomplished by applying static load onto the muscle body of the quadriceps and the hamstrings. The MLR has the ability to vary the loads on the individual heads of the quadriceps and the hamstrings as well as the ratio of quadriceps to hamstrings loads; therefore it will help in determining the effects of each head of the muscles on both PF and tibiofemoral (TF) kinematics. The rig will also aid in better understanding the change in knee joint motion due to different muscle weakness.

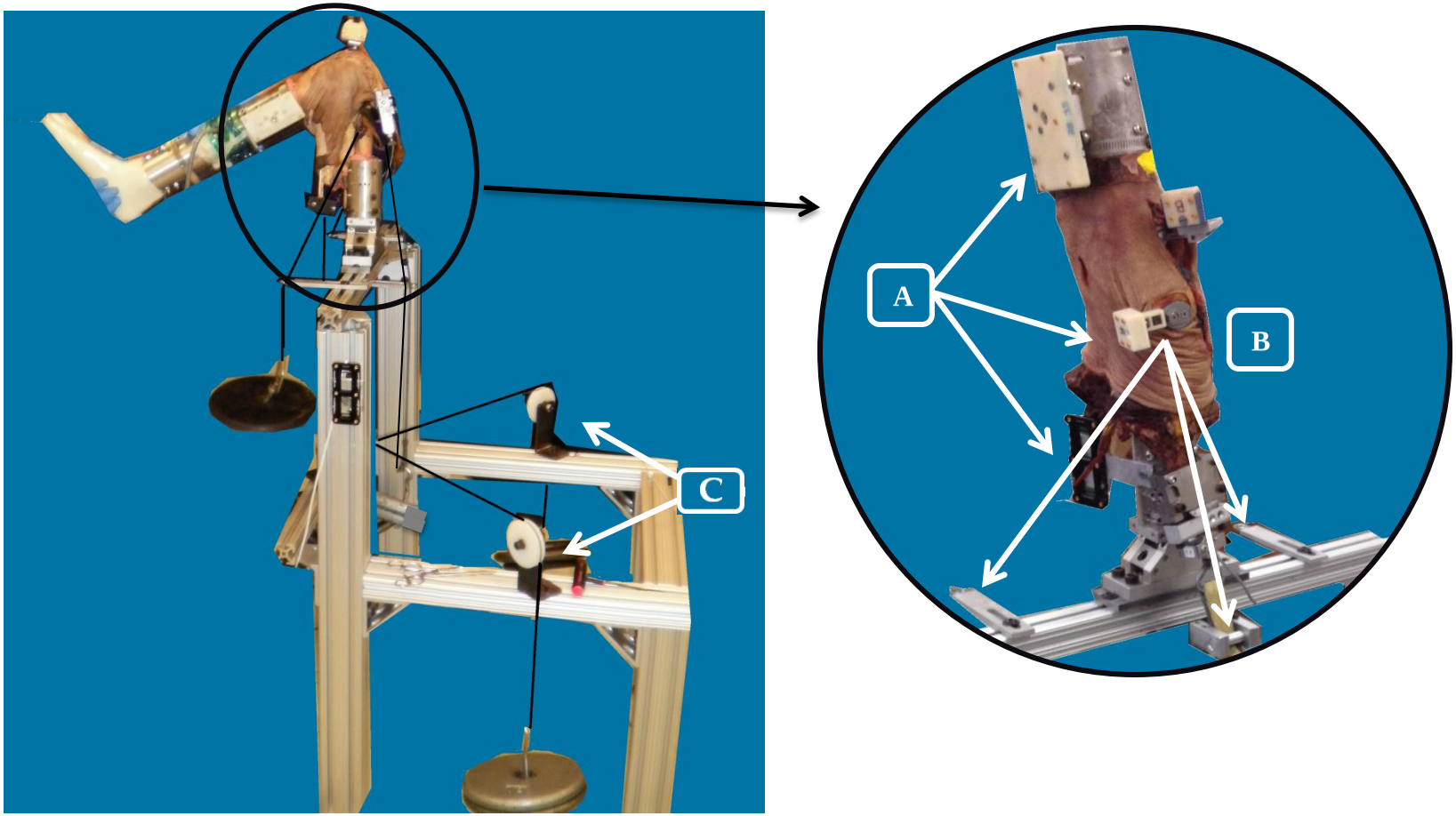


**Figure 3.1: The muscle loading rig with the femur rigidly attached to the MLR in an inverted position with: A) motion tacking array, B) arrows showing the line of action of the individual muscles of the quadriceps (from left to right: VL, RF&VI, and VM), and C) pulleys to redirect the load of the hamstrings.**

### 3.2.2. Testing Protocol

Fourteen fresh frozen cadaveric knees (age: 67 ± 14 years; BMI: 23.8 ± 4.4) were thawed at room temperature and dissected. The femur and tibia were sectioned 22.5 cm proximal and 17.5 cm distal to the epicondular axis and potted in aluminum fixture tubes with bone cement. All the soft tissue within 10 cm of the joint line was left intact. Except the muscle bodies of the quadriceps and hamstrings, all soft tissue and musculature beyond 10 cm from the joint line were completely removed. Individual heads of the quadriceps (VM, VL, RF, and VI) and the hamstrings (BF and SM) were identified, separated, and clamped individually with the exception of clamping the RF and the VI together. The knees were mounted onto the MLR and the steel plates and pulleys were adjusted to match the orientation reported by Farahmand *et al.* [8]. The kinematics of each bone were recorded using an Optotrak 3020 motion capture system (Northern Digital, Ontario) and anatomical landmarks on the femur and patella were digitized to describe the kinematics using a three-axis orthogonal coordinate system adapted to the PF joint [77].

Manual manipulation (Ma) and motor manipulation (Mo) protocols were used to test the hypothesis of this study. The first consisted of manual manipulation of the knee through the range of flexion by the author while in the second the knee was dynamically flexed through the range of flexion using the MLR motor that was attached to the muscle body of the RF and VI. Eight knees were tested using the first protocol, and eight knees were tested using the second protocol. Two specimens were tested using both manual and dynamic protocols. For the Ma protocol, a total load of 175N was applied to the quadriceps based on previous studies [27, 59, 78] for both the single line and physiological based loading configuration. Four different loading configurations were tested:

1) Normal Manual Manipulation (NMa): physiological based loading with each head of the

quadriceps loaded with a percentage of the total load based on the muscle mean physiological cross sectional area [8, 40].

2) Single Line Manual Manipulation (SMa): single line of action loading simulation with the total load applied through the RF and VI only.
3) Weak Vastus Medialis (WVM): simulating the extreme case of weakness in the VM while keeping minimal tension on the muscle.
4) Weak Vastus Lateralis (WVL): shifting the load from the VL to both the VM and the RF and VI to explore the effect of extreme VL weakness.

The percentage of the total load applied to the individual muscles of the quadriceps for each configuration is presented in Table 3.1

**Table 3.1: Percentage of the load on the individual heads of the quadriceps for each loading configuration.**

| Configuration | RF and VI | VM | VL |
|---|---|---|---|
| **Normal (NL)** | 35% | 25% | 40% |
| **Single Line (SMA)** | 100% | 0% | 0% |
| **Weak Vastus Medialis (WVM)** | 40% | 5% | 55% |
| **Weak Vastus Lateralis (WVL)** | 50% | 35% | 15% |

For the dynamic simulation, a Nema 34 stepper motor (Danahar automation, Illinoi) was attached to the RF and VI clamp. A 300 lb load cell (Transducer Technique, California) was connected in line with the motor to measure the load applied on the knee by the RF and VI. The motor position for 20° and 120° knee flexion were recorded for each specimen. The knee was flexed between the two position for two different simulations: 1) no loads on the VM and the VL (SMo), and 2) the VM and the VL statically loaded with 30 N and 55 N respectively (NMo)

based on their physiological cross sectional area [8, 40] . A total load of 175 N was split equally between the two hamstrings to provide a flexion moment during both Ma and Mo simulations.

### 3.2.3. Data Analysis

The NMo and the NMa cycles were set as the base patellar flexion, shift, tilt, and spin for both Mo and Ma simulations. An excursion (deviation from the base cycle) was calculated for the each cycle (SMa, WVM, and WVL for the Ma, SMo for the Mo) relative to their respective physiological based cycle. The range of motion for each tracking kinematic was measured for every cycle. The means and standard deviations was calculated for both protocols separately and a one way ANOVA was performed to find any significant differences ($p<0.05$) between the SMA, WVM, WVL for the MP, the SMO for the MO and their respective normal cycle in 15 degrees increments.

## 3.3. Results

The data for the four patellar tracking kinematics measured in this study showed no difference between the flexion and extension cycle therefore both cycles were averaged together. The four patellar tracking measures for the four loading configurations (NMa, SMa, WVL, WVM) were averaged for the eight specimens and are presented in Figure 3.2 to illustrate the overall motion of the patella for each cycle, although the results and discussion describe the kinematics as the relative difference from the physiological based cycle (NMa and NMo).

### 3.3.1. Loading Configuration

During both the manual manipulation and the dynamic simulation, the patellar flexion of the SMA loading configuration was more extended than that of the NMa loading configuration throughout the entire cycle, although the difference was only significant from extension to early

flexion (15°-60°) (Figure 3.3 A) . The largest difference in PF flexion was 2.75° for Ma and 2.61° for Mo simulation occurring in early flexion around 15° (Table 3.2). As the knee flexed, the deviation from the physiological based loading configuration in both Ma and Mo decreased gradually until reaching a plateau around 85° where the SMA patella was slightly more extended than the ML patella (0.22° and 0.29° respectively). The patella had a slight medial shift for the SMa configuration compared to the NMa during the cycle, but the difference was only significant at 45° and 60° knee flexion (Figure 3.3 B, Table 3.2). On the other hand, in the Mo simulation, patellar glide during SMo had similar kinematics to that of the NMo. Patellar tilt for the SMA loading did not have a consistent deviation from ML in early flexion (15°-30°) across specimens, although past 45° knee flexion the difference across specimen became more consistent and was significant at 45°, 60°, and 75° knee flexion (Figure 3.3 C). There was no significant difference in patellar rotation between the two conditions for both dynamic simulation and manual manipulation (Figure 3.3 D). A summary of the average difference and standard deviation along with statistical difference between the single line of action and the normal configuration for both protocols is presented in Table 3.2. Little to no difference was observed in PF kinematics between the manual and motor manipulation for the two knees that received both protocols (Appendix A).

### 3.3.2. Muscle Weakness

Patellar flexion and tilt showed no significant difference when simulating either a WVM or a WVL (Figure 3.4A, C). The WVM resulted in a lateral patellar tracking while the WVL caused a more medial tracking to the NMa (Figure 3.4 B). The difference between the NMa and each the WVM and WVL for patellar glide was significant from early flexion until 90°. Patellar rotation was also affected by muscle weakness where a WVM consistently rotated the patella

externally (around 0.42°) throughout the cycle compare to the NMa simulation (Figure 3.4 D). On the other hand, the data showed that the patella was on average 0.53° more internally rotated during WVL when compared to that of the NMa. The change in patellar rotation tracking was small but significant differences were detected between the NMa and both the WVM and WVL. Table 3.3 summarizes the difference in patellar flexion, tilt, rotation and glide for both WVM and WVL from the physiological based loading (NMa).

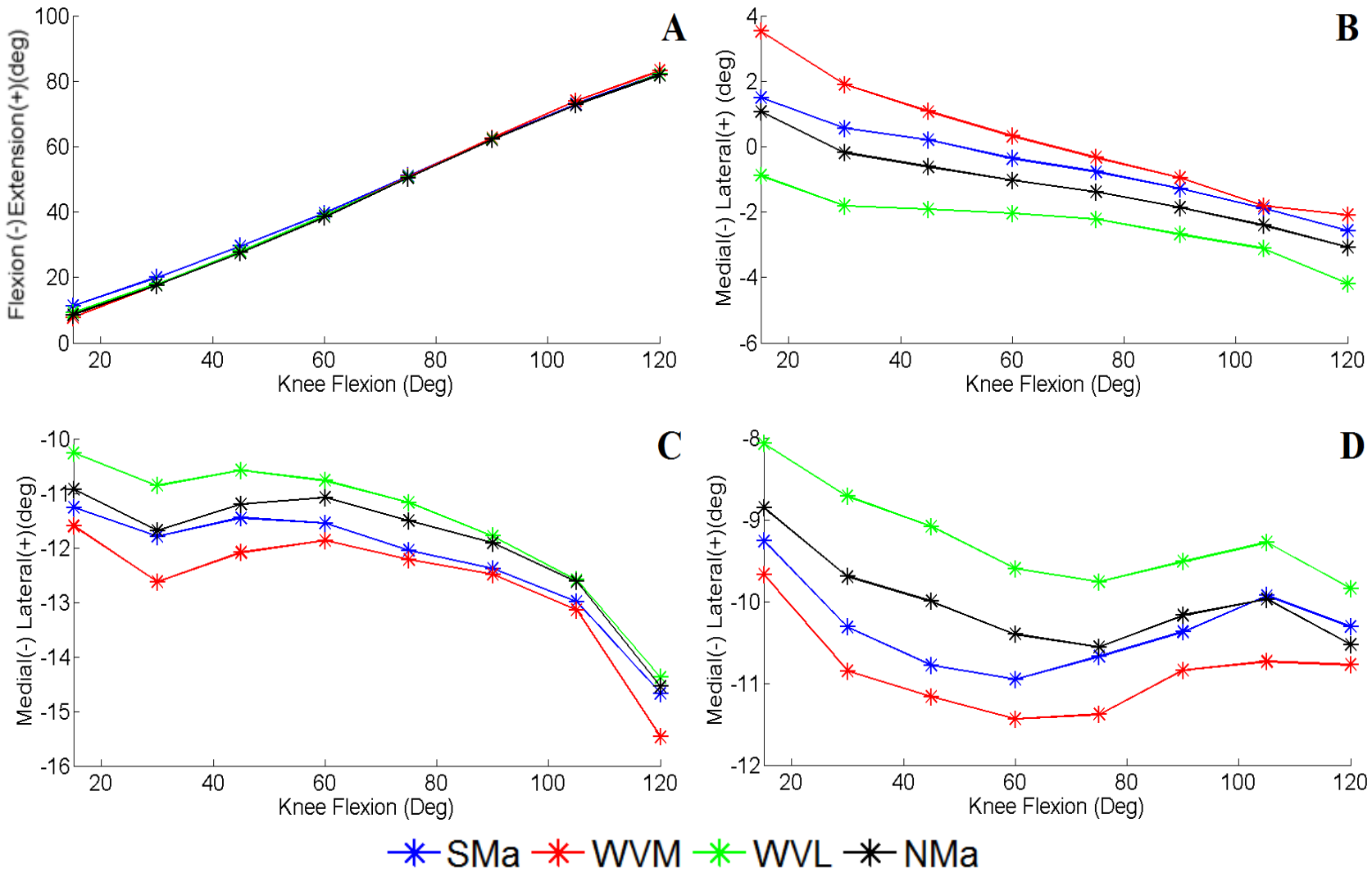


**Figure 3.2: Mean kinematics of the four patellar tracking measures: A) flexion, B) shift, C) tilt, and D) rotation for the SMa (Blue), WVM (Red), WVL (green), and NMa (black) in the three-axis orthogonal coordinate system before normalization.**

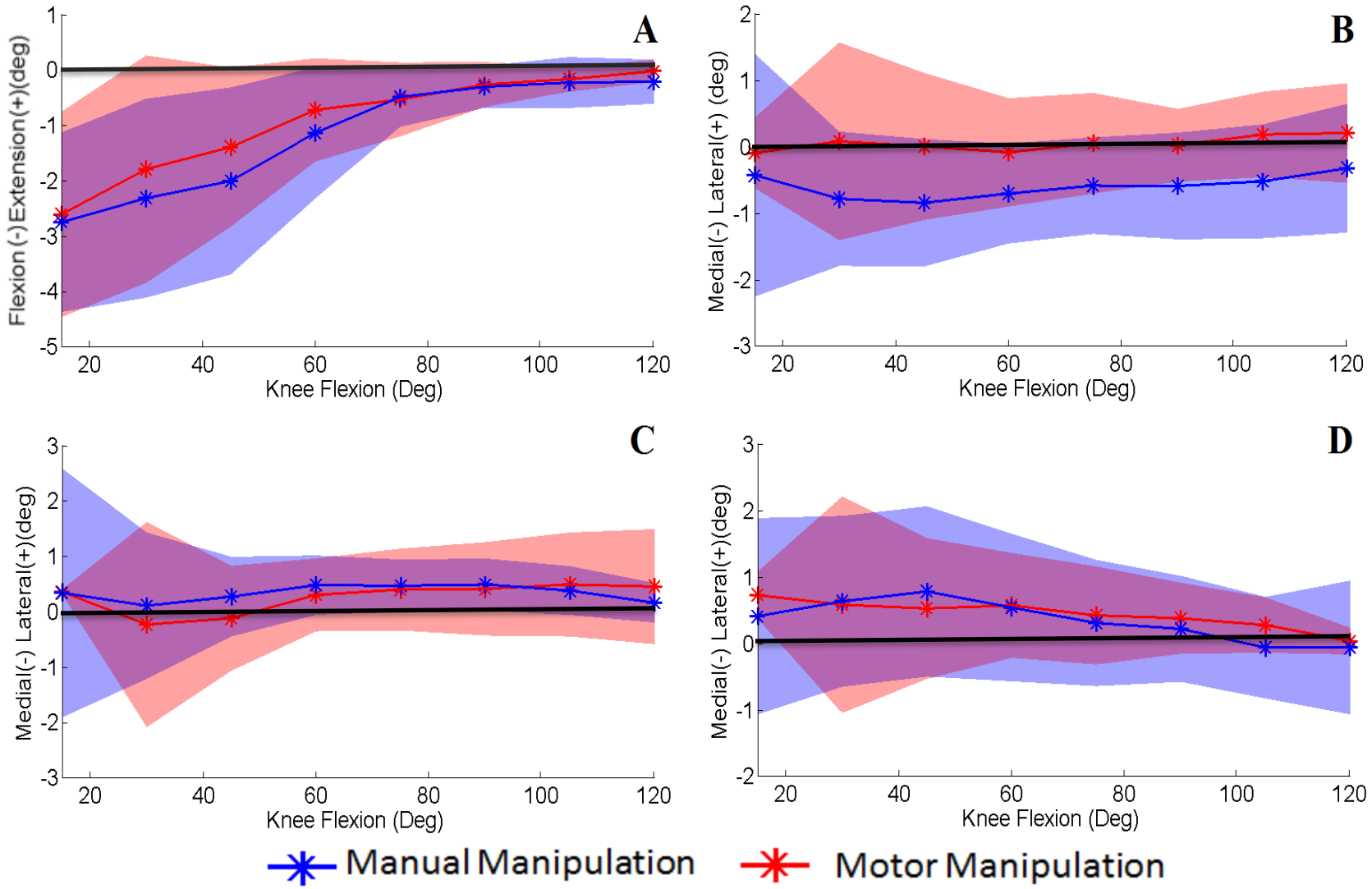


**Figure 3.3: Mean difference of the four patellar tracking measures: A) flexion, B) shift, C) tilt, and D) rotation for the manual manipulation (Blue), and motor manipulation (Red) relative to their respective physiological based loading cycle. The shaded area represents the data point within ±1 standard deviation.**

**Table 3.2: Mean and standard deviation of the difference between single line loading and multiple line loading configurations (SL-NMa) for both manual manipulation and dynamic simulation across the eight specimens**

| | Flexion (Deg) | | Rotation (Deg) | | Tilt (Deg) | | Glide (mm) | |
|---|---|---|---|---|---|---|---|---|
| | Manual | Dynamic | Manual | Dynamic | Manual | Dynamic | Manual | Dynamic |
| **15°** | -2.8 ± 1.6* | -2.6 ±1.8* | 0.4 ± 1.5 | 0.7 ± 0.4 | 0.3 ± 2.2 | 0.4 ± 0.1 | -0.4 ± 1.8 | -0.1 ± 0.5 |
| **30°** | -2.3 ± 1.8* | -1.8 ± 2.1* | 0.6 ± 1.3 | 0.6 ± 1.6 | 0.1 ± 1.3 | 0.2 ± 1.8 | -0.8 ± 1.0 | -0.1 ± 1.4 |
| **45°** | -2.0 ± 1.7* | -1.4 ± 1.4* | 0.8 ± 1.3 | 0.5 ± 1.1 | 0.3 ± 0.7 | 0.3 ± 0.9 | -0.8 ± 1.0* | 0.0 ± 1.1 |
| **60°** | -1.1 ± 1.2* | -.7 ± 0.9* | 0.5 ± 1.1 | 0.6 ± 0.8 | 0.5 ± 0.5* | 0.3 ± 0.7 | -0.7 ± 0.7* | -0.1 ± 0.8 |
| **75°** | -0.5 ± 0.5 | -0.5 ± 0.7 | 0.3 ± 1.0 | 0.4 ± 0.7 | 0.5 ± 0.4* | 0.4 ± 0.7 | -0.6 ± 0.7 | 0.1 ± 0.7 |
| **90°** | -0.3 ± 0.4 | -0.3 ± 0.4 | 0.2 ± 0.8 | 0.4 ± 0.5 | 0.5 ± 0.4* | 0.4 ± 0.8 | -0.6 ± 0.8 | 0.0 ± 0.5 |
| **105°** | -0.2 ± 0.5 | -0.2 ± 0.2 | -0.1 ± 0.8 | 0.3 ± 0.4 | 0.4 ± 0.4 | 0.5 ± 0.9 | -0.5 ± 0.9 | 0.2 ± 0.6 |
| **120°** | -0.2 ± 0.4 | 0.0 ± 0.2 | -0.1 ± 1.0 | 0.0 ± 0.2 | 0.2 ± 0.3 | 0.5 ± 1.0 | -0.3 ± 1.0 | -0.2 ± 0.7 |

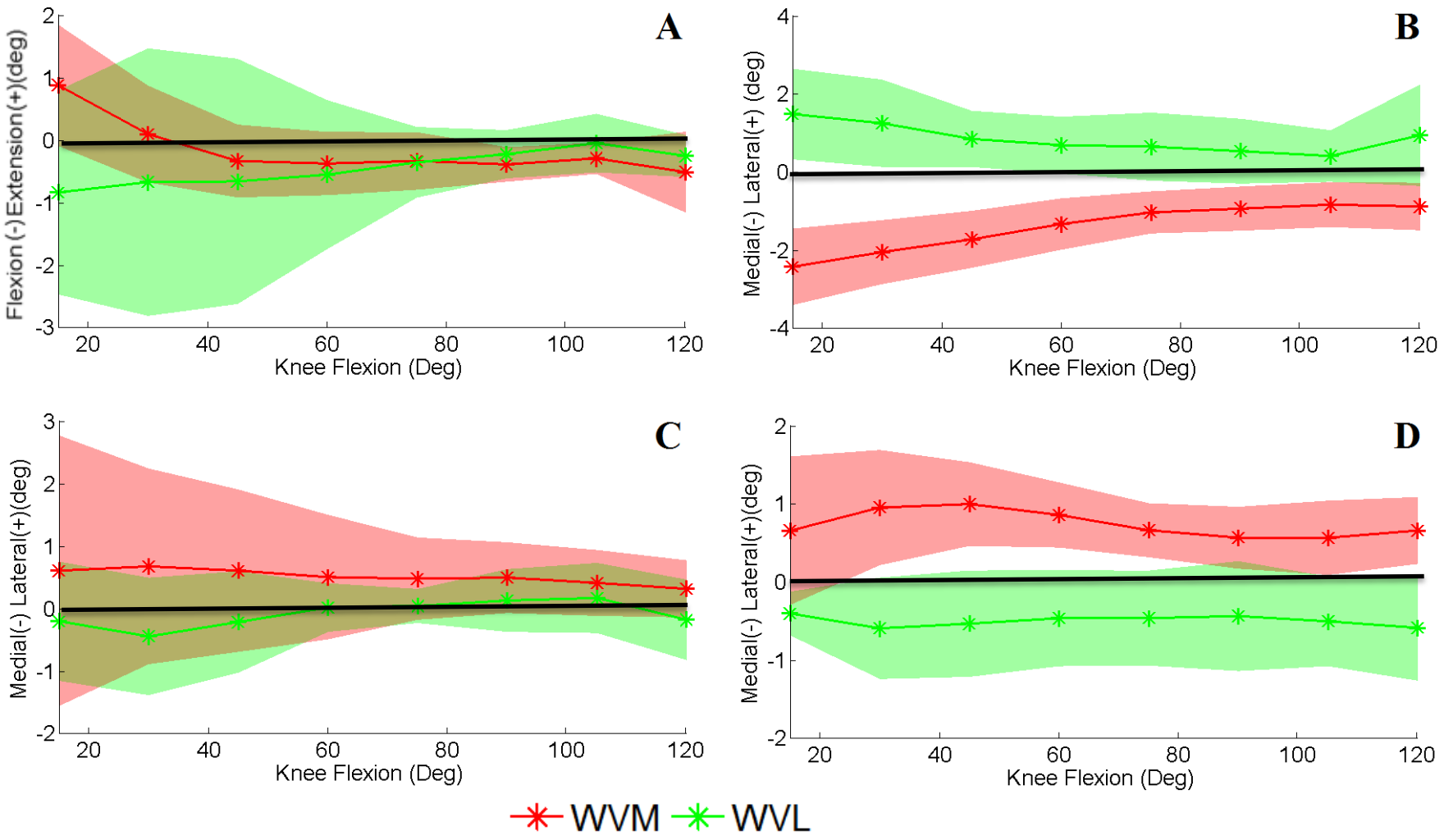


**Figure 3.4 Mean difference of the four patellar tracking measures: A) flexion, B) shift, C) tilt, and D) rotation for WVM (Green) and WVL (Red) during manual manipulation relative to their physiological based loading cycle (NMa). The shaded area represents the data point within ±1 standard deviation.**

**Table 3.3: Mean and standard deviation of the difference between NMA and each, WVM and WVL (WVM-NMa, (WVL-NMa) for both manual manipulation and dynamic simulation across the eight specimens**

| | Flexion (Deg) | | Rotation (Deg) | | Tilt (Deg) | | Glide (mm) | |
|---|---|---|---|---|---|---|---|---|
| | WVM | WVL | WVM | WVL | WVM | WVL | WVM | WVL |
| **15** | -0.9 ± 0.9 | 0.8 ± 1.6 | -0.6 ± 0.9* | 0.4 ± 0.2* | -0.6 ± 2.1 | 0.2 ± 0.9 | 2.4 ± 0.9* | -1.4 ± 1.1* |
| **30** | -0.1 ± 0.7 | 0.6 ± 2.1 | -0.9 ± 0.7* | 0.5 ± 0.6* | -0.6 ± 1.5 | 0.4 ± 0.9 | 2.1 ± 0.8* | -1.2 ± 1.1* |
| **45** | 0.3 ± 0.5 | 0.6 ± 1.9 | -0.9 ± 0.5* | 0.5 ± 0.6* | -0.6 ± 1.3 | 0.2 ± 0.8 | 1.7 ± 0.7* | -0.8 ± 0.7* |
| **60** | 0.4 ± 0.5 | 0.5 ± 2.0 | -0.8 ± 0.4* | 0.4 ± 0.6* | -0.5 ± 0.9 | -0.0 ± 0.9 | 1.3 ± 0.6* | -0.6 ± 0.6* |
| **75** | 0.3 ± 0.4 | 0.3 ± 0.5 | -0.6 ± 0.3* | 0.4 ± 0.6* | -0.4 ± 0.6 | -0.0 ± 0.2 | 1.0 ± 0.4* | -0.6 ± 0.8* |
| **90** | 0.4 ± 0.2 | 0.2 ± 0.3 | -0.5 ± 0.4* | 0.4 ± 0.7* | -0.49 ± 0.6 | -0.1 ± 0.5 | 0.9 ± 0.6* | -0.5 ± 0.8* |
| **105** | 0.3 ± 0.2 | 0.1 ± 0.4 | -0.5 ± 0.4* | 0.5 ± 0.5* | -0.4 ± 0.5 | -0.2 ± 0.5 | 0.8 ± 0.5 | -0.4 ± 0.6 |
| **120** | 0.5 ± 0.6 | 0.2 ± 0.3 | -0.6 ± 0.4* | 0.5 ± 0.6* | -0.3 ± 0.4 | 0.2 ± 0.6 | 0.8 ± 0.6 | -0.9 ± 1.3 |

## 3.4. Discussion

This study examined the effects of different loading configurations (single line loading and physiological based loading) and muscle weakness (VM and VL weakness) on PF kinematics.

### 3.4.1. Single Line vs. Physiological Based Loading

The difference in patellar flexion between single and multiple lines of action could be explained by the non-parallel forces to the axis of the femur generated from the VM and the VL. These two muscle loads are applied from the superior portion of the patella causing a flexion moment that significantly increases the flexion angle of the patella relative to the femur in the NMa and NMo configuration. Past 60° TF flexion, the PF contact area increases with flexion as the patella enters the trochlear groove [38, 79, 80]. This geometric interaction between the patella and the femur restrain the patella and decrease the effect of the posterior force applied by the VM and VL which in turn minimize the difference between the single line loading and physiological based loading configuration for both Ma and MO. The standard deviation observed between SMa, SMo, and their respective physiological based loading configurations were largest at extension and decreased with flexion as the patella entered the trochlear groove, suggesting that the anatomy of the knee plays a bigger role in constraining patellar flexion than muscle loading during deep flexion.

In the manual manipulation, the patella was more internally tilted and had a more medial position in the SMa compare to the NMa configuration. This shift and rotation can be explained by the force applied on the VL which is larger than the one applied on the VM (70 N compared to 43 N). The absence of the VM and VL loading vector shifted the resultant vector of the SMa configuration and induced more internal rotation and medial shift compared to the NMa configuration when the VM and VL were loaded. The largest difference in patella glide was

observed between 30-60° between the SMa and NMa configuration. This was expected because the medial retinaculae is the primary restraint against lateral patellar shifts in extension [32], which is lax around 25°. Additionally, the patella is not firmly seated in the trochlear groove which decreases the resistance for lateral displacement in this flexion range [28]. The increase in external tilt of the patella seen in the ML configuration is a result of the difference in the VM and VL loads coupled with the glide and tilt kinematics of the patella as it enters the trochlear groove. As the patella shifts laterally, it rides on the lateral edge of the groove causing an external rotation of the patella relative to the femur. No significant differences were observed in patellar rotation between the two loading configurations for both manual and motor manipulations. This indicates that the force applied by the VM muscle body was sufficient to counteract the force of the VL muscle body.

The difference between the SMA and ML for the four patellar tracking measures in this study had similar patterns to the ones presented by Powers *et al.* [13], although the differences between the two loading configurations was smaller in this study. This could be explained by the specimen preparation method: While Powers *et al.* removed all the skin, subcutaneous fat, the fibula at its articulation with the tibia, and all musculature from the tibia as well as the posterior femur, this study left the skin, soft tissue, and the entire musculature within 10 cm of the join line intact. The excess skin soft tissue and musculature could have confined the PF joint and reduced the effects of the VM and VL forces.

Variation in PF tracking between the two loading configurations (single line and physiological based) were larger during the Ma compared to the Mo, especially in the frontal plane kinematics. Small differences were seen between the SMo and NMo frontal plane resultant force vector due to the large load applied on the RF and VI during Mo resulting in the small

variation in the frontal plane kinematics between the two cycles (Figure 3.5 A). In the sagittal plane the resultant force for the SMo still differed from that of NMo but the difference was smaller than the one observed between SMa and NMa which explains the decrease in patellar flexion difference between the two cases (Figure 3.5 B).

### 3.4.2. Muscle weakness vs. Physiological Based loading

The effect of weakness in the VM and VL on PF kinematics was also investigated in this study to give an insight on their contribution on patellar stability. Patellar flexion was not affected by weakness in either the VM or the VL, which was expected since the resultant force in the sagittal plane for both WVM and WVM had similar orientation to that of the ML configuration (Figure 3.7). Significant differences were observed in patellar rotation during WVM and WVL simulations compared to the normal, which could be explained by the locations of the attachment sites of the VM and VL. The VM and the VL attach to the superomedial and superolateral edge of the patella respectively (Fig. 3.6). Therefore, in WVM, where the load on the VM is decreased; the force applied through the VL will induce an abduction moment about the axis through the center of the patella resulting in a significant increase in patellar abduction rotation. The opposite is true for the WVL, where the VL load is decreased; inducing an adduction moment that rotates the patella internally compared to the normal configuration. Patellar shift for WVM and WVL was significantly different from the ML across the whole flexion cycle, but the largest variation was seen between 15-45° TF flexion. The large variation in this flexion range can be attributed to the decrease in patellar restraint against medial and lateral forces which was reported to be the lowest in this range [28, 31]. In addition, weakness in the VM shifted the patellar glide laterally, while weakness in the VL shifted the patella medially. Similar results were observed by Goh *et al.*, and Saki *et al.* [18, 27]. Maltracking of the patella

has been attributed to PF pain and patellar dislocation [18, 81, 82], and based on the results of this study weakness in the VM could be a one of the reason of these PF disorders. The results support the findings of the study by Goh *et al.* [18] stating that releasing the VL, a procedure performed to realign the VL force vector, could correct the maltracking induced by the weakness in the VM. In addition, strengthening the VM will medially shift the resultant force that results in a more medialized position of the patellar and could reduce anterior knee pain.

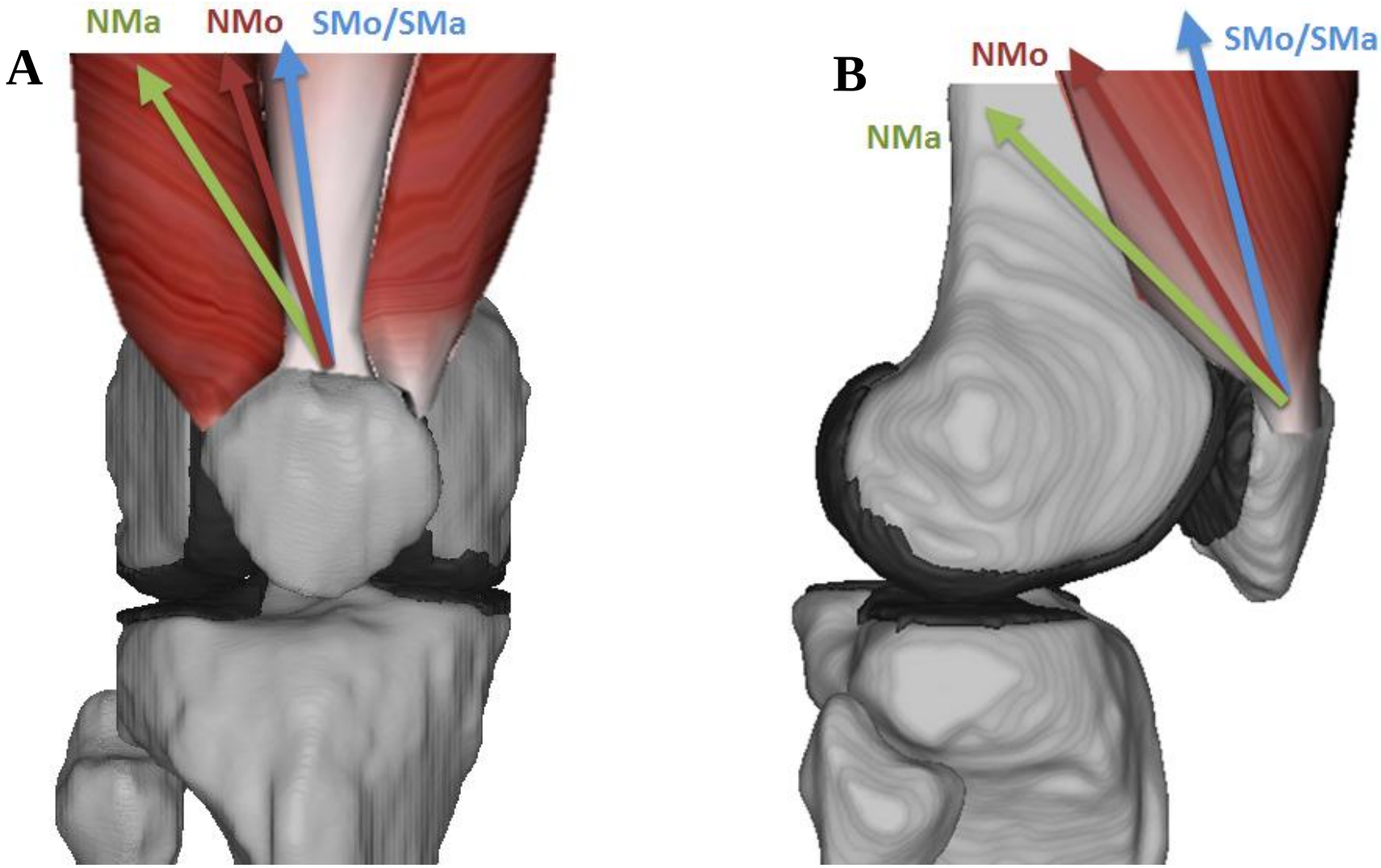


**Figure 3.5: Approximate Mo and calculated Ma directions of the resultant magnitude of the muscle resultant force for the four loading configurations; SMa and SMo (Blue), NMo (Red), and NMa (Green) in (A) the frontal plane, and (B) sagittal plane. The difference between NMa and SLA was 10° in the frontal plane and 26° in the sagittal plane.**

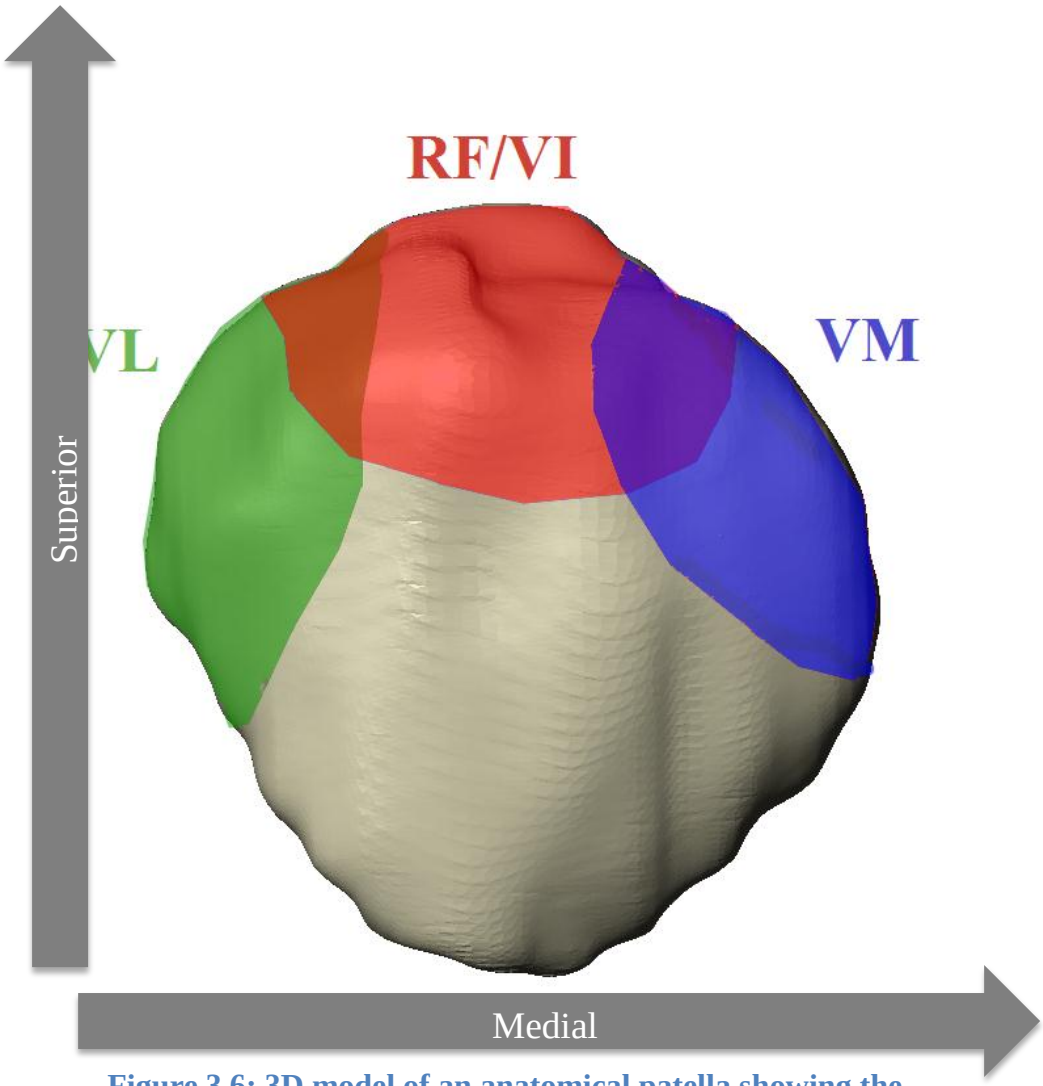


**Figure 3.6: 3D model of an anatomical patella showing the anatomical attachment cite area of each head of the quadriceps; RF & VI (red), VL (Green), and VM (Blue)**

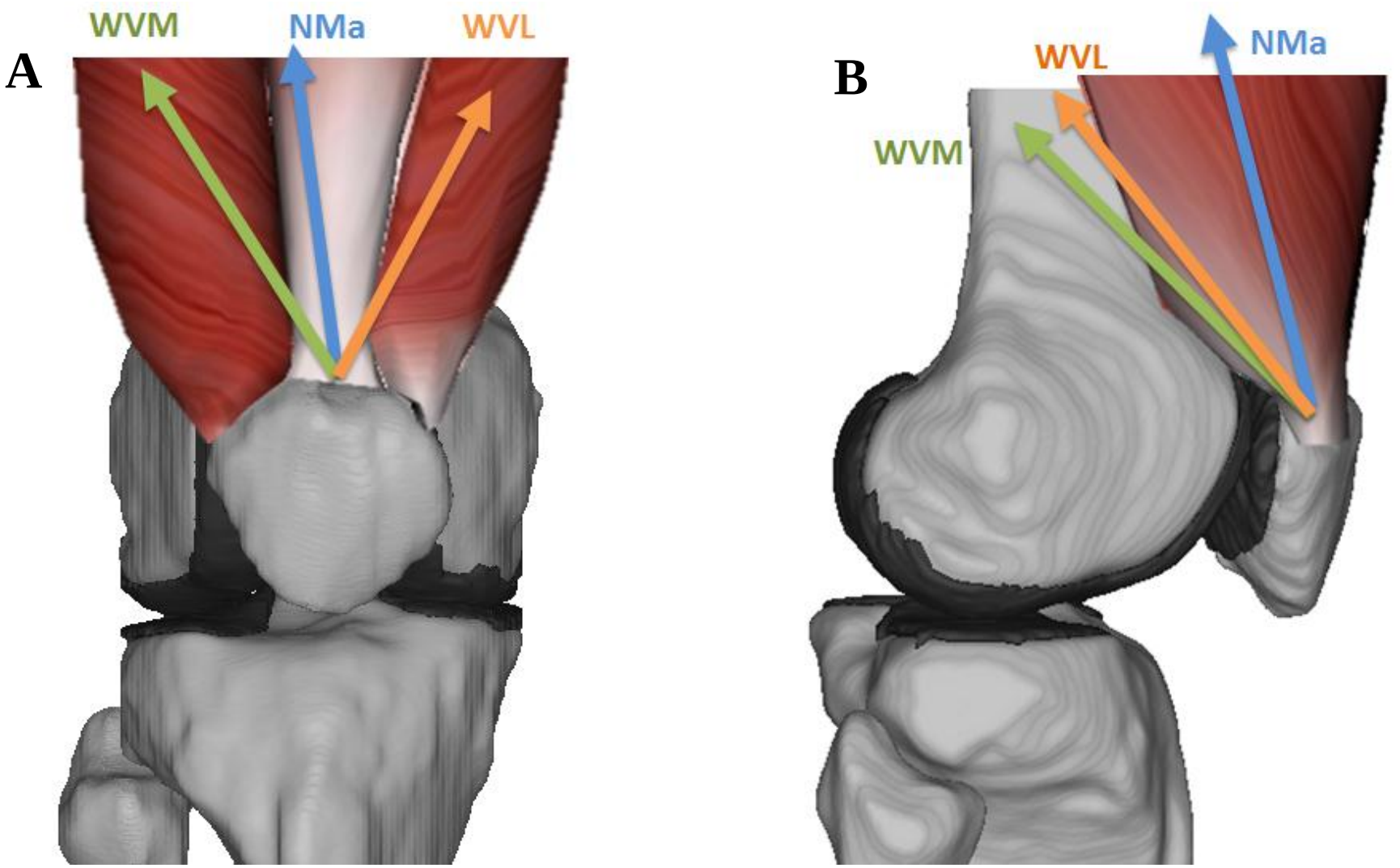


**Figure 3.7: Calculated resultant force vector direction of the muscle loading for the three loading configurations; ML (Blue), WVM (Red), and WVL (orange) in (A) the frontal plane, and (B) sagittal plane. The WVM and WVL are off the axis of the NMa by 17° lateral and 8° medial in the frontal plane and 26° and 22° in the sagittal plane respectively.**

## 3.5. Conclusion

The results of this study concur with the first hypothesis that the configuration used to load the extensor mechanism of the knee significantly affects the PF kinematics. Simulating the extensor mechanism as a single line of action muscle reduces the complexity of the loading configuration and could be used to draw conclusion of certain PF kinematics (rotation, shift) especially in deeper flexion. On the other hand, physiological based loading should be used when examining PF contact area, pathologies, and kinematics that are affected by the sagittal plane loads (flexion, tilt). Similar kinematics to that of the physiological based loading were achieved during NMo by the addition of a small load to the VM and the VL suggesting that the addition of these minimal loads to *in vivo* dynamic simulation study could yield more similar PF kinematics to that of a physiological based loading compared to using a single line of action.

Both simulations that replicated VM or VL weakness in this study displayed maltracking in the PF joint especially patellar shift supporting the second hypothesis of this chapter. Based on these findings, weakness in the VM or the VL muscles could induce PF maltracking resulting in anterior knee pain and patellar dislocation.

# 4. The Effect of Different Hamstrings Loading Conditions on Tibiofemoral Lowest Point and IE Kinematics

## 4.1. Introduction

The hamstrings are an antagonist of the quadriceps and are the major flexor muscle group of the knee. The hamstrings, in addition to the anterior cruciate ligament, function as a restraint to anterior tibial translation [83]. *In vitro* studies descriptions of TF native knee kinematics are greatly varied [53, 54, 66]. Intra-specimen variability could be one cause of varied kinematics, but experimental setup and muscle loading conditions significantly influence kinematics. In addition, kinematics reported for *in vitro* studies are different than for *in vivo* studies. This difference is especially present with *in vitro* studies that utilize quadriceps dominant dynamic simulators and loading rigs that do not simulate the effects of the hamstrings [1, 73, 75, 84-86].

Higher anterior tibial translation in the natural knee and post-cam engagement at deeper flexion in the prosthetic knee compared to predicted results have been observed in ongoing studies at the Experimental Joint Biomechanics Research Laboratory with the Kansas Knee Simulator (KKS). The differences in the TF kinematics were attributed to the exclusion of a direct hamstrings simulation in the KKS and it was hypothesized that the inclusion of these muscles would result in more similar kinematics to the predicted and *in vivo* results. In addition, identifying the co-contraction ratio between the hamstrings and the quadriceps, the force and the orientation of the load that needed to be applied during the simulation was needed before making any modifications to the KKS.

The current study is the first step in quantifying the hamstrings moment arm and the effects of hamstrings loadings, which could aid in the development of simulation techniques and loading

parameters that improve current *in vitro* testing and produce more physiological kinematics. The purpose of this study was to identify *in vitro*, the effects of equal static hamstrings load on TF kinematics and quadriceps load, and compare the tracking measures from both hamstrings and no hamstrings loading scenarios to that of an *in vivo* study. It was hypothesized that the inclusion of hamstrings would decrease the internal rotation, anterior translation, as well as the overall range of motion throughout the entire flexion range. In addition the quadriceps load with the hamstrings loaded would increase unequally throughout the flexion cycle compared to the quadriceps load with no hamstrings loading. Identifying the impact of the hamstrings on TF kinematics will help understand the limitations and results variation between different studies. The results can also illustrate whether simulating *in vitro* testing with static hamstrings load could generate TF kinematics similar those observed *in vivo*.

## 4.2. Materials and Methods

### 4.2.1. Testing Protocol

Eight fresh frozen cadaveric knees (age: 67 ± 14 years; BMI: 23.8 ± 4.4) were thawed at room temperature. Each knee was MR imaged using an isotropic T2trufi3D sequence with (.5x.5x.5mm) voxel size. Sagittal plane images were manually segmented using solid modeling software (Simpleware, Virginia) to construct 3D anatomical models of the distal femur bone and cartilage. The knees were then dissected with the femur and tibia sectioned 22.5 cm proximal and 17.5 cm distal to the epicondylar axis and potted in aluminum fixture tubes with bone cement. All the soft tissue within 10 cm of the joint line was left intact. Except for the muscle bodies of the quadriceps and the hamstring, all soft tissue and musculature beyond 10 cm from the joint line was completely removed. The RF and the VI of the quadriceps and the BF and SM of the hamstrings were identified, separated, and clamped using custom made metal clamps.

The knees were mounted with the femur rigidly attached in an inverted position onto the MLR with the tibia unconstrained as described in the Chapter 3 (Figure 4.1). A Nema 34 stepper Motor (Danahar automation, Illinoi) attached to the quadriceps tendon and the motor rotation corresponding to 20° and 120° TF flexion were recorded for each specimen. The two positions were used to dynamically move the knee between the two flexion angles. A 300 lb load cell (Transducer Technique, California) was connected in line with the quadriceps to measure the load applied during the cycle.

The kinematics of each bone were recorded using an Optotrak 3020 motion capture system (Northern Digital, Ontario) and anatomical landmarks on the femur and the tibia were digitized to describe the kinematics using a three-axis orthogonal coordinate system [87, 88]. Hexahedral meshes of the femur bone and cartilage were constructed using Hypermesh (Altair, Alabama). The meshed femoral bone was transformed into the tibial coordinate system and the lowest point (LP) of the medial and lateral femoral condyle along the tibial superior-inferior (SI) direction were determined at each flexion angle and projected onto the surface of the tibia for visualization.

The kinematics were measured as the knee flexed between 20° and 120° knee flexion for two different loading conditions:

1. Quadriceps only (QO): No load on the hamstrings.
2. Quadriceps and hamstrings (QH): 40 lb static dead weights shared equally on both hamstrings (BF and SM).

Two specimens were additionally tested with different percentages of the total load on the medial

and lateral hamstrings (SM and BF respectively) to get preliminary data on the effects of variable medial and lateral hamstrings loads on the kinematics. A summary of these loading configurations along with the main two protocols is presented in Table 4.1.

### 4.2.2. Data Analysis

The quadriceps only cycle was set as the base TF kinematics measured for each individual knee. The excursion (deviation from the base cycle) was calculated for the QH cycle and SMH, SML, BFL, and BFH when applicable from the QO cycle. The mean and standard deviation for the medial and lateral LP positions and range of motion, and TF rotation were calculated across specimens in 10° increments. A paired student t-test was performed to find any significant differences ($p<0.05$) between the two main loading configuration (QH and QO) throughout the flexion range in 10° increments.

**Table 4.1: Percentages of the total load applied on each head of the hamstrings for the different loading configurations**

| Configuration | BF | SM |
|---|---|---|
| **Quadriceps only (QO)** | 0 | 0 |
| **Quadriceps and hamstrings (QH)** | 50% | 50% |
| **High SM load I (SML)** | 37.5% | 62.5% |
| **High SM load II(SMH)** | 75% | 25% |
| **Lateral BF load I(BFL)** | 62.5% | 37.5% |
| **Lateral BF load II(BFH)** | 75% | 25% |

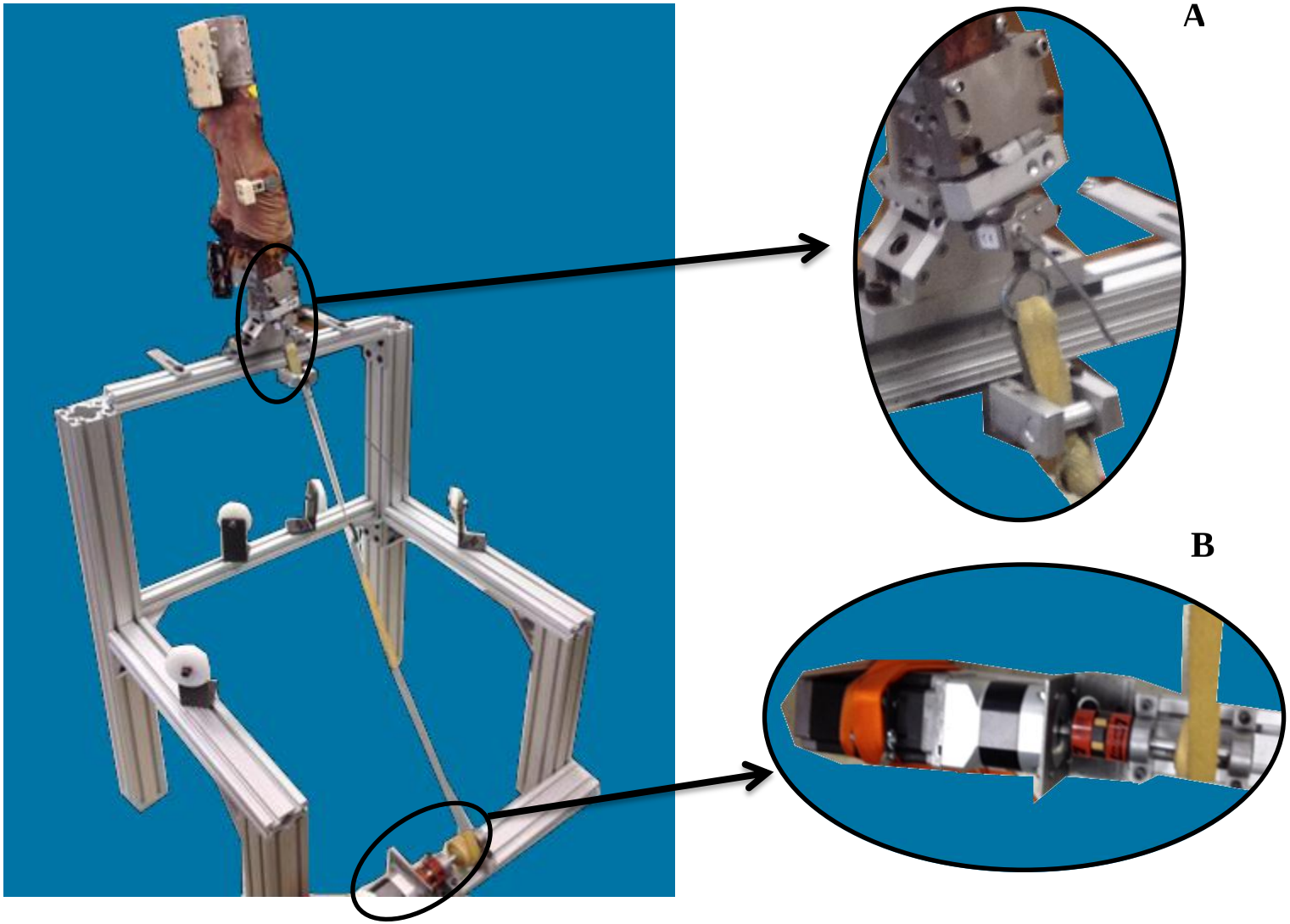


**Figure 4.1: Picture of the experimental setup with a cadaveric knee mounted on the MLR in an inverted position showing (A) 300 lb load cell to measure quadriceps load, and (B) Nema 34 motor in line with a gearbox and a coupler to move the knee dynamically through the range of flexion range between 10° and 120°.**

## 4.3. Results

The inclusion of hamstrings loading during the flexion cycle resulted in significant differences for the three measures that were tracked in this study (TF IE rotation, medial and lateral LP) (Figure 4.2). The medial LP during QH simulation was slightly more anterior (0.7 mm on average) compared with QO simulation during early flexion (from 10-40°). However, past 60° the calculated medial LP of the QH configuration was more posterior compared to that of the QO simulation with the largest difference of 1.1±1.7 mm occurring at 80° flexion (Figure 4.3). The medial LP difference between the two cases was significantly different only between 10-40° knee flexion (Table 4.2).

The addition of 180 N antagonist loads on the hamstrings reduced the posterior femur translation of the lateral LP significantly throughout the cycle except at 10° (Table 4.2). The difference in the posterior translation between the two cases was small at full extension (0.2 ±0.8 mm) and increased until 40° where a posterior difference of approximately 5.2 mm remained consistent throughout the rest of the flexion range (Figure 4.3 A).

The inclusion of hamstrings also affected the femoral IE rotation causing the femur to be more internally rotated compare to the QO simulation throughout the entire flexion range tested (Figure 4.3 B). The femur rotation during QH started similarly to that of the QO between 10° and 20°. As the knee went into flexion the difference between the two cycles increased gradually until 100° TF flexion where it decreased for the rest of the cycle. The difference reached its maximum of 6.89° more external at 100° TF flexion. Except for 10° and 20° flexion, the calculated change in femoral IE rotation was significantly different through the whole cycle (Table 4.2).

Quadriceps load varied significantly between the two loading configurations (Figure 4.4). A similar pattern to that of the IE kinematics variation was observed for the quadriceps load where the difference in quadriceps loads was minimal at full extension and increased gradually as the knee went through flexion until hitting a plateau close to 100° flexion with the quadriceps loaded with an extra 70 lb in the QH configuration compare to that of the QO configuration.

The ranges of motion of both the medial and lateral LP decreased when the hamstrings were loaded (Figure 4.5). The decrease was from 7.2 mm to 5.6 mm for the medial LP and from 8.90 mm to 7.9 mm for the lateral LP. The average change in the range of motion was calculated to be 1.6 mm and 0.8 mm for the medial and lateral LP respectively (Figure 4.5).

Changing the percentage of the hamstrings load between the medial and lateral heads of the hamstrings for two knees affected the three tracking measures of this study (Figure 4.6). The observed differences in the kinematics were variable and dependent on the loading condition. Loading the SM with a higher percentage of the total hamstrings load resulted in similar IE tracking for the SML while the SMH configuration externally rotated the femur compare to the QO simulation (Figure 4.6 C). For the high lateral hamstrings loading, the difference in IE rotation tracking was similar to that observed between the QO and QH simulations. The magnitude of the difference increased with the increase of the load percentage applied on the BF (Figure 4.6).

Similar overall shapes of the differences between the QO and the different hamstrings loading configurations for the lateral LP were observed (Figure 4.6 A). The lateral LP difference was minimal for the SMH and increased as loading percentage shifted from the medial to the lateral side. The increase in loading percentage on the SM shifted the lateral LP difference

posteriorly compare to that of the QH difference (Figure 4.6 B), and the medial LP more posteriorly at 50° and 65° flexion for SML and SMH respectively compared to 73° for the QH cycle. On the other hand the medial LP shifted more anteriorly throughout the whole flexion range for the BFL and BFH compared to that of the QH cycle. Higher percentage of load on the BF resulted in an increase in the anterior shift of the medial LP.

**Table 4.2: Difference of the three tracking measures (medial and lateral LP, and IE rotation,) between QH and QO [QH-QO] for the eight specimens.**

| Flexion (Deg) | Medial LP (mm) | Lateral LP (mm) | IE (Deg) |
|---|---|---|---|
| 10 | 0.4 ± 0.5 * | 0.2 ± 0.8 | -0.5 ± 1.3 |
| 20 | 0.7 ± 0.8 | 1.8 ± 1.3 * | 1.1 ± 1.6 |
| 30 | 0.7 ± 0.7 * | 4.0 ± 2.0 * | 3.2 ± 2.1 * |
| 40 | 0.8 ± 0.8 * | 5.2 ± 2.7 * | 4.3 ± 2.6 * |
| 50 | 0.3 ± 0.7 | 5.2 ± 2.7 * | 4.9 ± 2.9 * |
| 60 | -0.1 ± 0.8 | 5.1 ± 2.5 * | 5.4 ± 3.0 * |
| 70 | -0.7 ± 1.0 | 4.9 ± 2.1 * | 5.9 ± 3.1 * |
| 80 | -1.0 ± 1.6 | 5.1 ± 2.1 * | 6.4 ± 3.2 * |
| 90 | -0.9 ± 1.3 | 5.5 ± 1.7 * | 6.7 ± 3.0 * |
| 100 | -0.8 ± 1.3 | 5.7 ± 1.6 * | 6.8 ± 3.1 * |
| 110 | 0.1 ± 1.0 | 5.4 ± 1.5 * | 5.4 ± 2.0 * |
| 120 | 0.4 ± .07 | 4.2 ± 1.8 * | 3.9 ± 2.2 * |

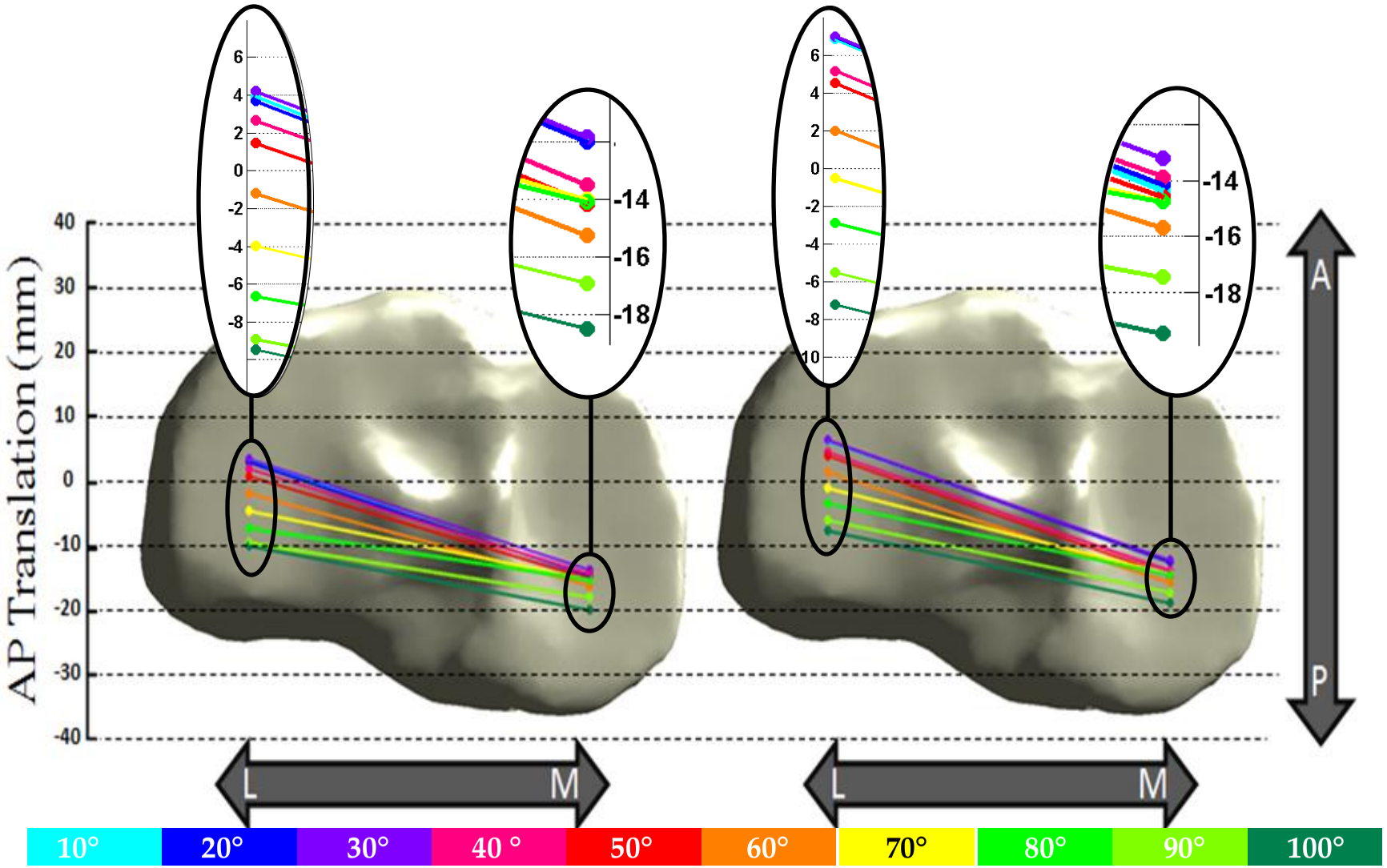


**Figure 4.2: Top view of the tibia showing the average medial and lateral lowest point for Quad only and (Left) Quad and hamstrings simulation (Right) from 10° to 120°.**

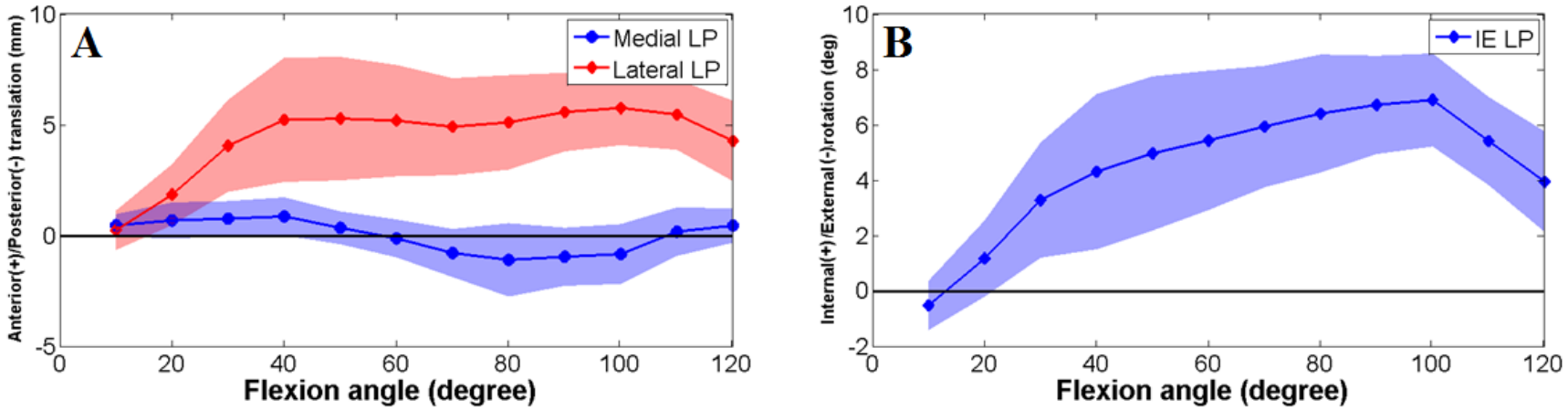


**Figure 4.3: Mean difference between QH and QO [QH-QO] for (A) medial (blue) and lateral (red) lowest point kinematics and (B) internal/external rotation with the shaded area as ±1 standard deviation for the eight specimens.**

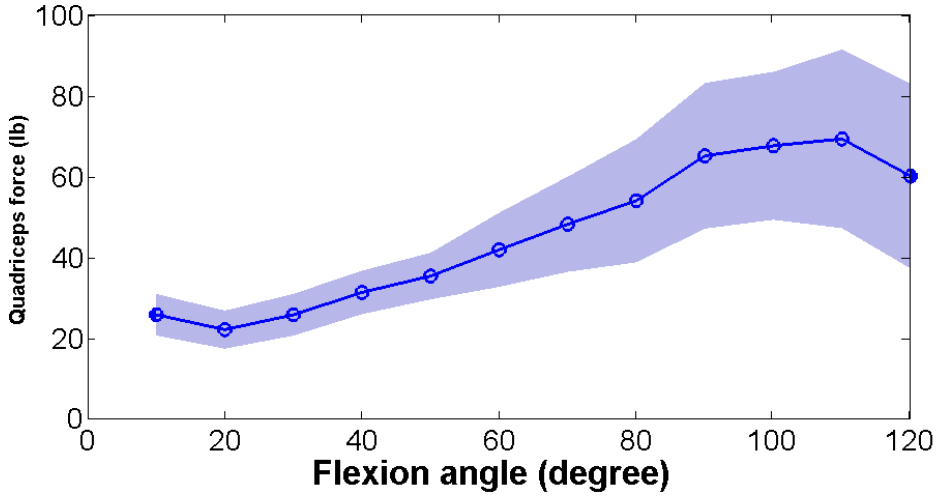


**Figure 4.4: Quadriceps load difference between QO and QH configuration [QH-QO] with the shaded area as ±1 standard deviation. Statistical significant differences were found across the entire flexion range.**

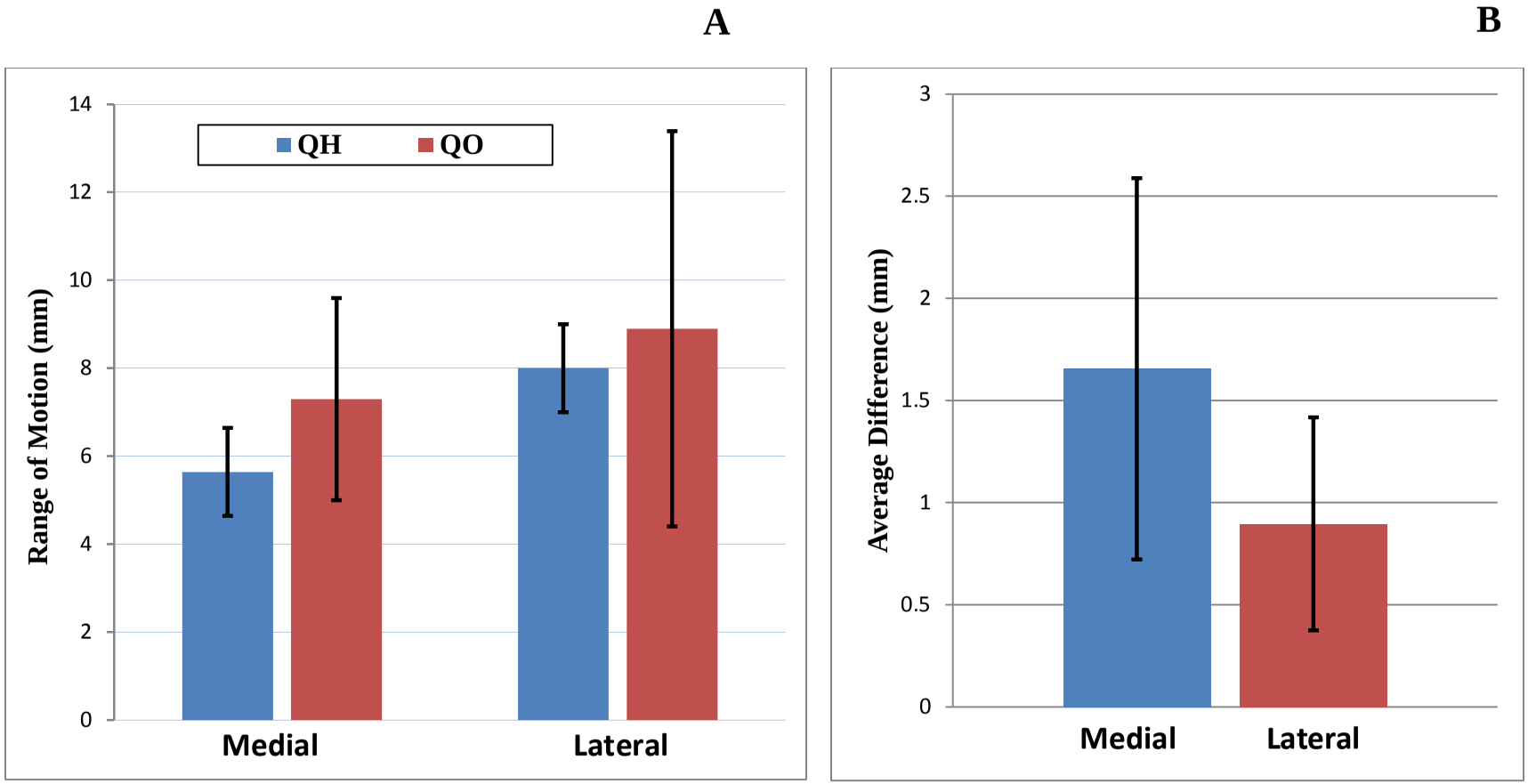


**Figure 4.5: Tibiofemoral AP translation; (A) range of motion of the medial and lateral lowest point for both QH (blue) and QO (red), and (B) average difference between QH and QO [QH-QO] for the medial (blue) and lateral (red) LP.**

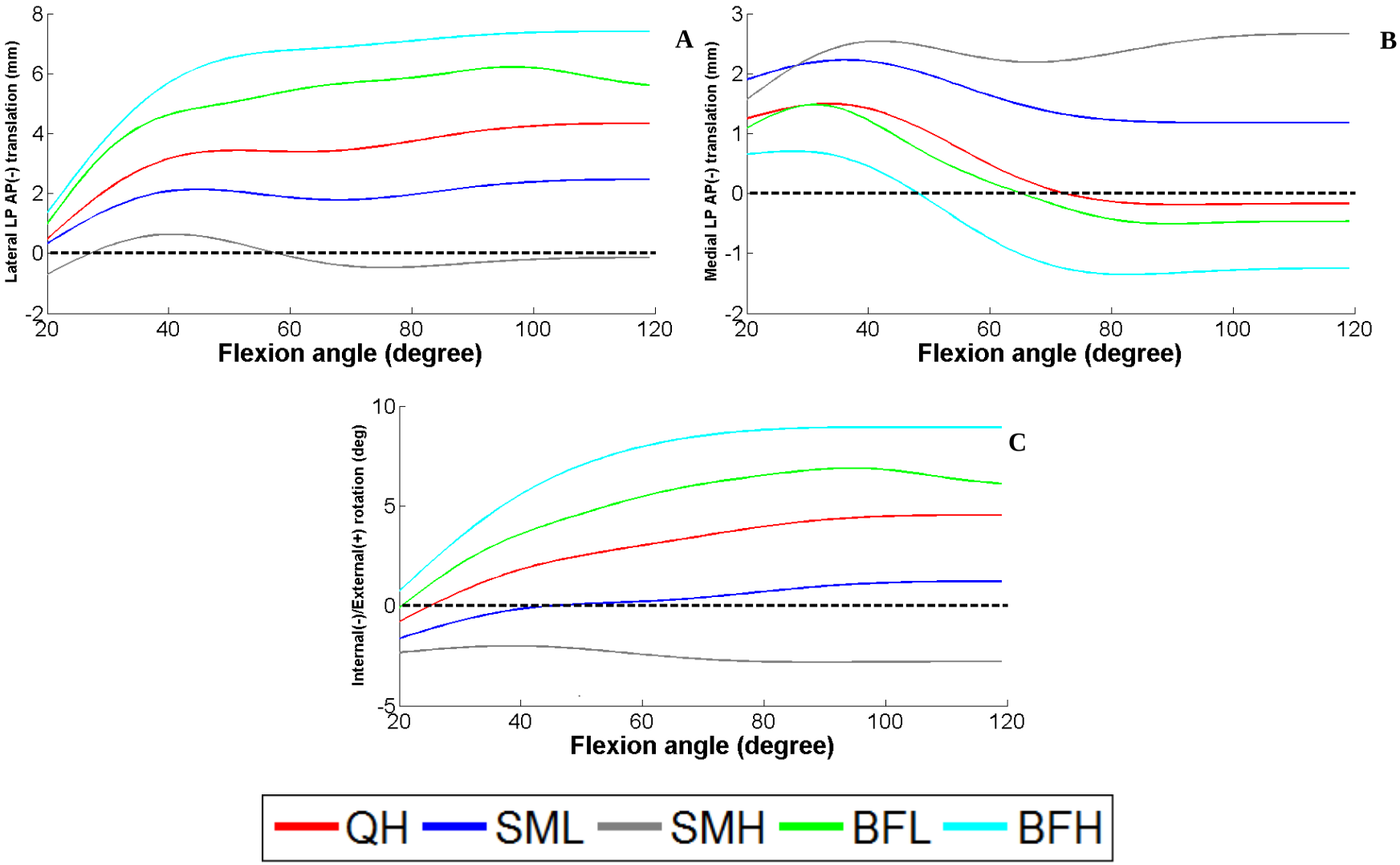


**Figure 4.6: Difference of tibiofemoral kinematic from QO during each loading configuration; QH (red), SML(blue), SMH (gray), BFL (green), and BFH (cyan) for: (A) lateral lowest point, (B) medial lowest point, and (C) internal/external rotation**

## 4.4. Discussion

The influence of different hamstrings loadings on TF kinematics was investigated in this study. Significant differences were observed for the TF IE rotation, and both medial and lateral LP kinematics between the two loading conditions. Based on the results of this study, the hypothesis that the inclusion of hamstrings loads during *in vitro* simulation would change the kinematics cannot be refuted.

The static equal load on the SM and the BF translated and rotated the femur anteriorly and externally relative to the tibia compared to the kinematics acquired from not loading the two muscles. The results of this study suggest that the addition of a posterior force directly through the hamstrings can reduce and limit tibial anterior translation and internal rotation in quadriceps dominant simulations. The effects of the added hamstrings load was minimal during early flexion and increased as the knee flexed beyond 35°. This could be explained primarily by the increase in the moment arms of both SM and BF muscles as the knee flexed [89]. Another explanation is the knee range of motion itself, as it has been reported that the knee is tightest at full extension and only allows small relative movement between the femur and the tibia [58]. The increase in the hamstrings moment arms with flexion is also the primary reason for the increase in variation in quadriceps load between the QO and QH, since the hamstrings loads were held constant throughout the entire flexion cycle. Loading the hamstrings was also successful in reducing both the medial and lateral LP, and IE rotation range of motion leading to the assumption that the knee is tighter when the hamstrings are loaded.

Tibial internal rotation was significantly decreased when the hamstrings were loaded. This study along with other studies [52, 66, 90] that have reported reduction in tibial internal rotation have isometrically loaded the hamstrings, therefore this reduction in tibial internal rotation can

just be the effects of loading the medial and lateral hamstrings equally. The moment arm of the BF is larger than that of the SM because the lateral tibial plateau width is larger than that of the medial plateau [91], and the BF inserts onto the lateral side of the head of the fibula while the SM insert mainly into the horizontal groove on the posterior medial aspect of the medial condyle of the tibia [92]. This creates a larger moment for the BF in the coronal plane compared to the SM that causes an external tibial moment when coupled with the equal loading of the two muscles. This external moment could have caused the reduction in the tibial internal rotation. Examining the data from the two knees that were loaded with different medial and lateral hamstrings load percentages have shown that the SML loading configuration resulted in the smaller change in IE rotation while still reducing the tibial anterior translation. The ratio of medial to lateral hamstrings load in the SML configuration is approximately 3:2 which is similar to the ratio of the cross sectional area of these muscles reported by Wickiewicz et al [7]. This suggests that using a 3:2 load ratio between the medial and lateral hamstrings respectively could result in similar IE kinematics to that of no hamstrings while still limiting the anterior tibial translation.

An offset in the lowest point kinematics was seen between the current *in vitro* study and *in vivo* studies. This offset could be explained by the inconsistency in defining the tibial coordinate system as well as the center of the tibia between the studies. The medial and lateral LP were offset to start at 0 mm at 20° TF flexion to exclude the effects of the variable tibial origin and coordinate system (Figure 4.7). The magnitudes of the AP range of motion along with its path through the flexion cycle were similar to that of other *in vivo* studies [52, 54, 55, 66]. This suggests that inclusion of the hamstrings load during *in vitro* studies could lead to more physiological simulations along with more accurate results.

This study suffered from being an *in vitro* study and several limitations should be taken into consideration. No compressive load was applied on the knee other than the one applied by the quadriceps and hamstrings muscles. The dynamic simulation through the flexion range was simulated using an open chain configuration and did not include any ground reaction forces. As a result of the knee being inverted, the TF kinematics were affected by the additional flexion moment induced by the tibial apparatus weight that was largest at 90°. Muscle forces were another limitation of this study where the muscles were statically loaded based on previous studies and did not take into consideration specific activation time or co-contraction ratio to the quadriceps.

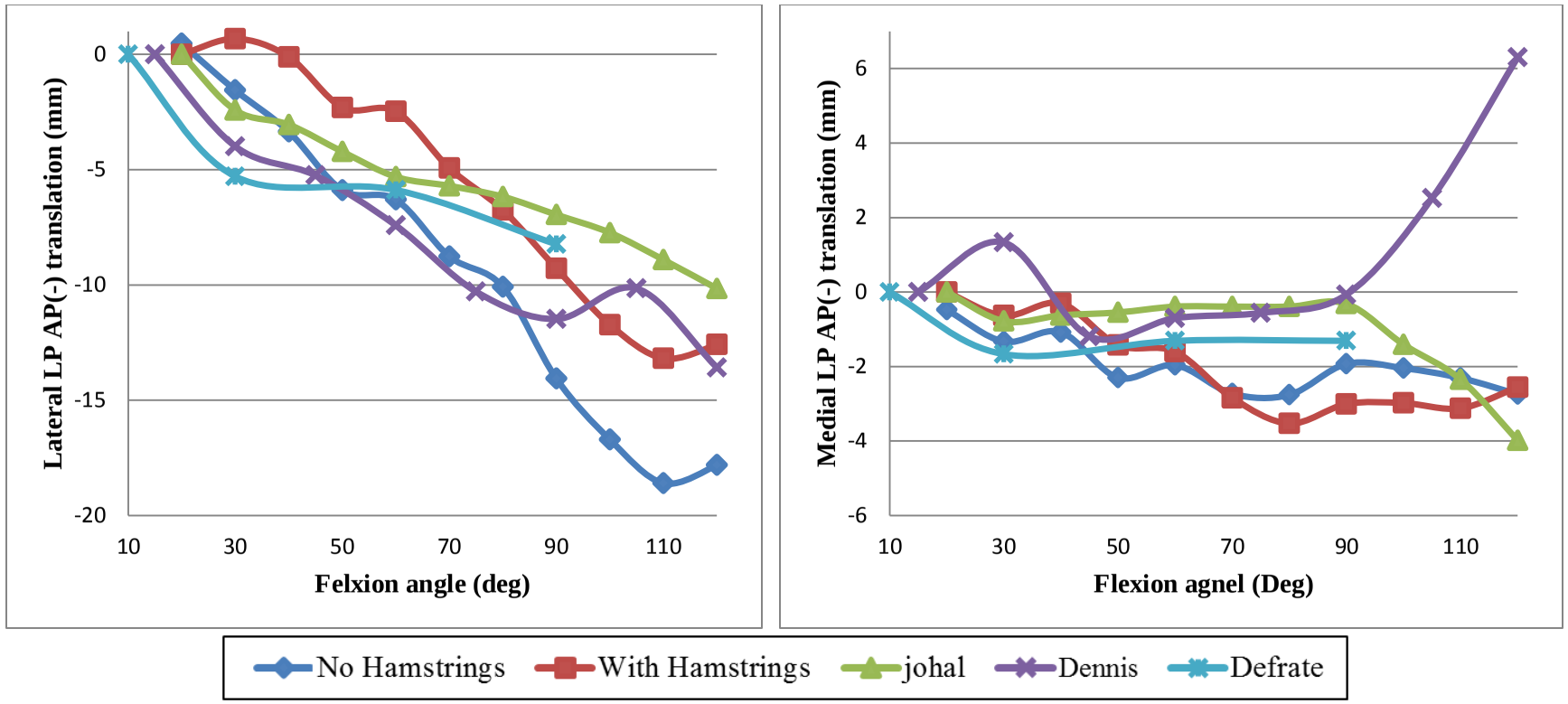


**Figure 4.7: Calculated lateral (Left) and medial (Right) LP kinematics for both hamstrings (red) and no hamstrings (blue) configuration compare to in-vivo studies ( Dennis *et al.* (purple), Defrate *et al.* (Cyan), and Johal *et al.* (green)) [88, 93, 94].**

## 4.5. Conclusion

This study supports the earlier hypothesis and demonstrates that the loading condition of the hamstrings significantly affects the TF kinematics and range of motion. The addition of hamstrings loading has been shown to decrease tibia anterior translations and could be incorporated into quadriceps dominant simulators to control these translations. Loading the hamstrings reduces tibia internal rotation, but it is unclear at this point whether this reduction is just a result of isometric loadings on the hamstrings. This study was the primary step in quantifying the effects of hamstrings on TF kinematics to determine how to incorporate them into quadriceps dominant dynamic knee simulators. Future studies are needed to investigate the effects of higher and lower hamstrings loads, and variable co-contraction ratio with the quadriceps on TF kinematics. The variation in kinematics due to different medial to lateral hamstrings load percentages need to be examined as well to determine the proper loading ratio between the two sides of the hamstrings. Lastly, future studies should examine the difference between statically and dynamically loading the hamstrings, based on its activation rate, on knee joint kinematics and kinetics. The addition of hamstrings loads during cadaveric simulations can be advantageous and could lead to simulations that better replicate physiological loading, but a full understanding of its effects on knee kinematics and hamstrings simulation techniques during *in vitro* simulation need to be developed before including it in dynamic knee simulators.

# 5. Conclusion and Future Work

The objective of this *in vivo* study was to quantify the changes in knee joint kinematics caused by changes in loading configurations of the quadriceps and the hamstrings. This will help identify the tracking measures that are most affected by the loading configuration. A second objective was to measure the variation in PF kinematics cause by weakness in the vastus lateralis or medialis. The study demonstrated that patellar flexion, shift and tilt were significantly affected by the change in the loading configuration of the quadriceps. Simulating the quadriceps as a single line of action decreased the patellar flexion angle, shifted and tilted the patella laterally and externally relative to physiological based loading of the quadriceps. Weakness in the VM and VL significantly varied the PF kinematics especially patellar shift and tilt. A more medialized position of the patellar with an increase in external tilt was observed when simulating a weakness in the VM. The opposite was true when simulating a weakness in the vastus lateralis. The inclusion of a statically isometric load on the hamstrings during *in vitro* simulation limited anterior tibial translation. This decrease in anterior translation was accompanied with a reduction in TF internal rotation but it is unclear at this point whether this reduction is just the influence of loading the medial and the lateral side equally.

There are a few limitations to this research that should be addressed in future studies. The knee was moved by the author through the range of flexion in the manual manipulation which could introduce inconsistencies in the applied force that could affect PF kinematics. The 175 N weight used to load the quadriceps in Chapter 3 was chosen to avoid muscle rupture at the cable attachment. This load is substantially lower than the one used in other studies as well as the true physiological load, which could also affect PF kinematics. Another limitation of this research was that the quadriceps in Chapter 3 and the hamstrings in Chapter 4 were simulated using a

static weight throughout the entire flexion cycle. This loading method assumes that the ratio of the individual quadriceps heads load stays consistent with flexion for Chapter 3, and that the hamstrings is always firing with the same force for Chapter 4.

The results of this research have implications for both clinical and *in vitro* studies. Chapter 3 indicated that weakness in the VM and lateralis results in maltracking of the patella which correlates weakness in these muscles to anterior knee pain. Rehabilitation exercises that focus on strengthening these muscles especially after invasive surgery like total knee arthoplasty is recommended to reduce anterior knee pain and provide more stability to the PF joint. This study has shown that knee joint kinematics is highly dependent on the loading configuration used during *in vitro* testing. Single line of action loading of the quadriceps muscle is sufficient when examining patellar rotation and shift but physiological based loading should be implemented when investigating flexion and tilt such as surgical techniques and implant which are affected by sagittal plane load. Increase in anterior tibial translation has been observed in quadriceps driven simulations. This study has shown that the inclusion of hamstrings loads during quadriceps driven simulations can limit the anterior tibial translation and create more physiological kinematics that are more consistent with what is observed clinically.

Future studies will address the limitation of this research and examine the effects of increasing the quadriceps and hamstrings loads as well as the difference when dynamically loading these muscles, based on their activation time, on knee joint kinematics. The effects of variable lateral to medial hamstrings load on TF kinematics and quantify hamstrings and quadriceps efficiency through the flexion cycle will also be investigated. The results obtained from this study along with future results will be used to establish *in vitro* testing parameters to

better replicate *in vivo* physiological conditions and make modification on the Kansas Knee Simulator in the Experimental Joint Biomechanics Research Laboratory.

# 6. References


1.Maletsky, L.P. and B.M. Hillberry, *Simulating dynamic activities using a five-axis knee simulator.* J Biomech Eng, 2005. **127**(1): p. 123-33.

2.Sauerland, E.K. and J.C.B. Grant, *Grant's dissector*. 12th ed1999, Philadelphia: Lippincott Williams & Wilkins. xviii, 329 p.

3.Gray, H., *Gray's anatomy*, ed. P.L.e. Williams and R.e. Warwick1973, London]: Longman.

4.Hartwig, W.C., *Fundamental anatomy*2008, Philadelphia: Wolters Kluwer Health/Lippincott Williams & Wilkins. ix, 417 p.

5.Tria, A.J., Jr., C.D. Johnson, and J.P. Zawadsky, *The popliteus tendon.* J Bone Joint Surg Am, 1989. **71**(5): p. 714-6.

6.Blazevich, A.J., N.D. Gill, and S. Zhou, *Intra- and intermuscular variation in human quadriceps femoris architecture assessed in vivo.* J Anat, 2006. **209**(3): p. 289-310.

7.Wickiewicz, T.L., R.R. Roy, P.L. Powell, and V.R. Edgerton, *Muscle architecture of the human lower limb.* Clin Orthop Relat Res, 1983(179): p. 275-83.

8.Farahmand, F., W. Senavongse, and A.A. Amis, *Quantitative study of the quadriceps muscles and trochlear groove geometry related to instability of the patellofemoral joint.* J Orthop Res, 1998. **16**(1): p. 136-43.

9..Wilson, N.A. and F.T. Sheehan, *Dynamic in vivo quadriceps lines-of-action.* J Biomech, 2010. **43**(11): p. 2106-13.

10.Waligora, A.C., N.A. Johanson, and B.E. Hirsch, *Clinical anatomy of the quadriceps femoris and extensor apparatus of the knee.* Clin Orthop Relat Res, 2009. **467**(12): p. 3297-306.

11.Sonin, A.H., S.W. Fitzgerald, M.E. Bresler, M.D. Kirsch, F.L. Hoff, and H. Friedman, *MR imaging appearance of the extensor mechanism of the knee: functional anatomy and injury patterns.* Radiographics, 1995. **15**(2): p. 367-82.

12.Staeubli, H.U., C. Bollmann, R. Kreutz, W. Becker, and W. Rauschning, *Quantification of intact quadriceps tendon, quadriceps tendon insertion, and suprapatellar fat pad: MR arthrography, anatomy, and cryosections in the sagittal plane.* AJR Am J Roentgenol, 1999. **173**(3): p. 691-8.

13.Powers, C.M., J.C. Lilley, and T.Q. Lee, *The effects of axial and multi-plane loading of the extensor mechanism on the patellofemoral joint.* Clin Biomech (Bristol, Avon), 1998. **13**(8): p. 616-624.

14.Andrikoula, S., A. Tokis, H.S. Vasiliadis, and A. Georgoulis, *The extensor mechanism of the knee joint: an anatomical study.* Knee Surg Sports Traumatol Arthrosc, 2006. **14**(3): p. 214-20.

15.Holt, G., T. Nunn, R.A. Allen, A.W. Forrester, and A. Gregori, *Variation of the vastus medialis obliquus insertion and its relevance to minimally invasive total knee arthroplasty.* J Arthroplasty, 2008. **23**(4): p. 600-4.

16.Hubbard, J.K., H.W. Sampson, and J.R. Elledge, *Prevalence and morphology of the vastus medialis oblique muscle in human cadavers.* Anat Rec, 1997. **249**(1): p. 135-42.

17.Peeler, J., J. Cooper, M.M. Porter, J.A. Thliveris, and J.E. Anderson, *Structural parameters of the vastus medialis muscle.* Clin Anat, 2005. **18**(4): p. 281-9.

18.Goh, J.C., P.Y. Lee, and K. Bose, *A cadaver study of the function of the oblique part of vastus medialis.* J Bone Joint Surg Br, 1995. **77**(2): p. 225-31.

19.Secko, M., M. Diaz, and L. Paladino, *Ultrasound diagnosis of quadriceps tendon tear in an uncooperative patient.* J Emerg Trauma Shock, 2011. **4**(4): p. 521-2.

20. Siwek, C.W. and J.P. Rao, *Ruptures of the extensor mechanism of the knee joint.* J Bone Joint Surg Am, 1981. **63**(6): p. 932-7.

21.Levy, M., J. Goldstein, and M. Rosner, *A method of repair for quadriceps tendon or patellar ligament (tendon) ruptures without cast immobilization. Preliminary report.* Clin Orthop Relat Res, 1987(218): p. 297-301.

22.Miskew, D.B., R.L. Pearson, and A.M. Pankovich, *Mersilene strip suture in repair of disruptions of the quadriceps and patellar tendons.* J Trauma, 1980. **20**(10): p. 867-72.

23.Wenzl, M.E., R. Kirchner, K. Seide, S. Strametz, and C. Jurgens, *Quadriceps tendon ruptures-is there a complete functional restitution?* Injury, 2004. **35**(9): p. 922-6.

24.Rougraff, B.T., C.C. Reeck, and J. Essenmacher, *Complete quadriceps tendon ruptures.* Orthopedics, 1996. **19**(6): p. 509-14.

25.Fairbank, J.C., P.B. Pynsent, J.A. van Poortvliet, and H. Phillips, *Mechanical factors in the incidence of knee pain in adolescents and young adults.* J Bone Joint Surg Br, 1984. **66**(5): p. 685-93.

26.Thomee, R., J. Augustsson, and J. Karlsson, *Patellofemoral pain syndrome: a review of current issues.* Sports Med, 1999. **28**(4): p. 245-62.

27.Sakai, N., Z.P. Luo, J.A. Rand, and K.N. An, *The influence of weakness in the vastus medialis oblique muscle on the patellofemoral joint: an in vitro biomechanical study.* Clin Biomech (Bristol, Avon), 2000. **15**(5): p. 335-9.

28.Senavongse, W., F. Farahmand, J. Jones, H. Andersen, A.M. Bull, and A.A. Amis, *Quantitative measurement of patellofemoral joint stability: force-displacement behavior of the human patella in vitro.* J Orthop Res, 2003. **21**(5): p. 780-6.

29.Makhsous, M., F. Lin, J.L. Koh, G.W. Nuber, and L.Q. Zhang, *In vivo and noninvasive load sharing among the vasti in patellar malalignment.* Med Sci Sports Exerc, 2004. **36**(10): p. 1768-75.

30.Goodfellow, J., D.S. Hungerford, and C. Woods, *Patello-femoral joint mechanics and pathology. 2. Chondromalacia patellae.* J Bone Joint Surg Br, 1976. **58**(3): p. 291-9.

31.Farahmand, F., M. Naghi Tahmasbi, and A. Amis, *The contribution of the medial retinaculum and quadriceps muscles to patellar lateral stability--an in-vitro study.* Knee, 2004. **11**(2): p. 89-94.

32.Senavongse, W. and A.A. Amis, *The effects of articular, retinacular, or muscular deficiencies on patellofemoral joint stability.* J Bone Joint Surg Br, 2005. **87**(4): p. 577-82.

33.Powers, C.M., *Rehabilitation of patellofemoral joint disorders: a critical review.* J Orthop Sports Phys Ther, 1998. **28**(5): p. 345-54.

34.McConnell, J., *Rehabilitation and nonoperative treatment of patellar instability.* Sports Med Arthrosc, 2007. **15**(2): p. 95-104.

35.Cowan, S.M., K.L. Bennell, and P.W. Hodges, *Therapeutic patellar taping changes the timing of vasti muscle activation in people with patellofemoral pain syndrome.* Clin J Sport Med, 2002. **12**(6): p. 339-47.

36.Ahmad, C.S., B.E. Stein, D. Matuz, and J.H. Henry, *Immediate surgical repair of the medial patellar stabilizers for acute patellar dislocation. A review of eight cases.* Am J Sports Med, 2000. **28**(6): p. 804-10.

37.Ostermeier, S., M. Holst, C. Hurschler, H. Windhagen, and C. Stukenborg-Colsman, *Dynamic measurement of patellofemoral kinematics and contact pressure after lateral retinacular release: an in vitro study.* Knee Surg Sports Traumatol Arthrosc, 2007. **15**(5): p. 547-54.

38.Wunschel, M., U. Leichtle, C. Obloh, N. Wulker, and O. Muller, *The effect of different quadriceps loading patterns on tibiofemoral joint kinematics and patellofemoral contact pressure during simulated partial weight-bearing knee flexion.* Knee Surg Sports Traumatol Arthrosc, 2011. **19**(7): p. 1099-106.

39.Koulouris, G. and D. Connell, *Hamstring muscle complex: an imaging review.* Radiographics, 2005. **25**(3): p. 571-86.

40.Wickiewicz, T.L., R.R. Roy, P.L. Powell, J.J. Perrine, and V.R. Edgerton, *Muscle architecture and force-velocity relationships in humans.* J Appl Physiol, 1984. **57**(2): p. 435-43.

41.Ali, K. and J.M. Leland, *Hamstring strains and tears in the athlete.* Clin Sports Med, 2012. **31**(2): p. 263-72.

42.Garrett, W.E., Jr., F.R. Rich, P.K. Nikolaou, and J.B. Vogler, 3rd, *Computed tomography of hamstring muscle strains.* Med Sci Sports Exerc, 1989. **21**(5): p. 506-14.

43. Jarvinen, T.A., M. Kaariainen, M. Jarvinen, and H. Kalimo, *Muscle strain injuries.* Curr Opin Rheumatol, 2000. **12**(2): p. 155-61.

44. Kujala, U.M., S. Orava, and M. Jarvinen, *Hamstring injuries. Current trends in treatment and prevention.* Sports Med, 1997. **23**(6): p. 397-404.

45.Garrett, W.E., Jr., *Muscle strain injuries: clinical and basic aspects.* Med Sci Sports Exerc, 1990. **22**(4): p. 436-43.

46.Woods, C., R.D. Hawkins, S. Maltby, M. Hulse, A. Thomas, and A. Hodson, *The Football Association Medical Research Programme: an audit of injuries in professional football--analysis of hamstring injuries.* Br J Sports Med, 2004. **38**(1): p. 36-41.

47.. Linklater, J.M., B. Hamilton, J. Carmichael, J. Orchard, and D.G. Wood, *Hamstring injuries: anatomy, imaging, and intervention.* Semin Musculoskelet Radiol, 2010. **14**(2): p. 131-61.

48.Mariani, C., F.E. Caldera, and W. Kim, *Ultrasound versus magnetic resonance imaging in the diagnosis of an acute hamstring tear.* PM R, 2012. **4**(2): p. 154-5.

49. Connell, D.A., M.E. Schneider-Kolsky, J.L. Hoving, F. Malara, R. Buchbinder, G. Koulouris, F. Burke, and C. Bass, *Longitudinal study comparing sonographic and MRI assessments of acute and healing hamstring injuries.* AJR Am J Roentgenol, 2004. **183**(4): p. 975-84.

50.Proske, U., D.L. Morgan, C.L. Brockett, and P. Percival, *Identifying athletes at risk of hamstring strains and how to protect them.* Clinical and Experimental Pharmacology and Physiology, 2004. **31**(8): p. 546-550.

51.Markolf, K.L., G. O'Neill, S.R. Jackson, and D.R. McAllister, *Effects of applied quadriceps and hamstrings muscle loads on forces in the anterior and posterior cruciate ligaments.* Am J Sports Med, 2004. **32**(5): p. 1144-9.

52.Li, G., T.W. Rudy, M. Sakane, A. Kanamori, C.B. Ma, and S.L. Woo, *The importance of quadriceps and hamstring muscle loading on knee kinematics and in-situ forces in the ACL.* J Biomech, 1999. **32**(4): p. 395-400.

53.MacWilliams, B.A., C. B, and E.Y. Chao. *Joint Simulation To Determine the Effects of Co-contration.* in *19th Annual Meetings of American Society of Biomechanics.* 1995. Stanford University, Stanford, CA.

54.Kwak, S.D., C.S. Ahmad, T.R. Gardner, R.P. Grelsamer, J.H. Henry, L. Blankevoort, G.A. Ateshian, and V.C. Mow, *Hamstrings and iliotibial band forces affect knee kinematics and contact pattern.* J Orthop Res, 2000. **18**(1): p. 101-8.

55.Victor, J., L. Labey, P. Wong, B. Innocenti, and J. Bellemans, *The influence of muscle load on tibiofemoral knee kinematics.* J Orthop Res, 2010. **28**(4): p. 419-28.

56.Biau, D.J., S. Katsahian, J. Kartus, A. Harilainen, J.A. Feller, M. Sajovic, L. Ejerhed, S. Zaffagnini, M. Ropke, and R. Nizard, *Patellar tendon versus hamstring tendon autografts for reconstructing the anterior cruciate ligament: a meta-analysis based on individual patient data.* Am J Sports Med, 2009. **37**(12): p. 2470-8.

57.Armour, T., L. Forwell, R. Litchfield, A. Kirkley, N. Amendola, and P.J. Fowler, *Isokinetic evaluation of internal/external tibial rotation strength after the use of hamstring tendons for anterior cruciate ligament reconstruction.* Am J Sports Med, 2004. **32**(7): p. 1639-43.

58.Blankevoort, L., R. Huiskes, and A. de Lange, *The envelope of passive knee joint motion.* J Biomech, 1988. **21**(9): p. 705-20.

59.Amis, A.A., W. Senavongse, and A.M. Bull, *Patellofemoral kinematics during knee flexion-extension: an in vitro study.* J Orthop Res, 2006. **24**(12): p. 2201-11.

60.Aglietti, P., R. Buzzi, G. Zaccherotti, and P. De Biase, *Patellar tendon versus doubled semitendinosus and gracilis tendons for anterior cruciate ligament reconstruction.* Am J Sports Med, 1994. **22**(2): p. 211-7; discussion 217-8.

61.Bollars, P., J.P. Luyckx, B. Innocenti, L. Labey, J. Victor, and J. Bellemans, *Femoral component loosening in high-flexion total knee replacement: an in vitro comparison of high-flexion versus conventional designs.* J Bone Joint Surg Br, 2011. **93**(10): p. 1355-61.

62.Taddei, P., E. Modena, T.M. Grupp, and S. Affatato, *Mobile or fixed unicompartmental knee prostheses? In-vitro wear assessments to solve this dilemma.* J Mech Behav Biomed Mater, 2011. **4**(8): p. 1936-46.

63.Iwaki, H., V. Pinskerova, and M.A. Freeman, *Tibiofemoral movement 1: the shapes and relative movements of the femur and tibia in the unloaded cadaver knee.* J Bone Joint Surg Br, 2000. **82**(8): p. 1189-95.

64.Bull, A.M., P.H. Earnshaw, A. Smith, M.V. Katchburian, A.N. Hassan, and A.A. Amis, *Intraoperative measurement of knee kinematics in reconstruction of the anterior cruciate ligament.* J Bone Joint Surg Br, 2002. **84**(7): p. 1075-81.

65.Grood, E.S., S.F. Stowers, and F.R. Noyes, *Limits of movement in the human knee. Effect of sectioning the posterior cruciate ligament and posterolateral structures.* J Bone Joint Surg Am, 1988. **70**(1): p. 88-97.

66.More, R.C., B.T. Karras, R. Neiman, D. Fritschy, S.L. Woo, and D.M. Daniel, *Hamstrings--an anterior cruciate ligament protagonist. An in vitro study.* Am J Sports Med, 1993. **21**(2): p. 231-7.

67.Clary C, Mane A, Reeve A, and L.P. Maletsky. *Knee kinematics during an in vitro simulated deep flexion squat.* in *ASME summer bioengineering conference*. 2007.

68.Lenz, N.M. and University of Kansas., *Simulation of a non-contact cutting maneuver to generate a realistic ACL injury in vitro*. p. 103 p.

69.Hamer, A. *A Static Knee-Loading apparatus.* in *3rd ANNUAL European Society of Biomechanics*. 1982. Nijmegen, Netherlands.

70.Fujie, H., K. Mabuchi, S.L. Woo, G.A. Livesay, S. Arai, and Y. Tsukamoto, *The use of robotics technology to study human joint kinematics: a new methodology.* J Biomech Eng, 1993. **115**(3): p. 211-7.

71.Rudy, T.W., G.A. Livesay, S.L. Woo, and F.H. Fu, *A combined robotic/universal force sensor approach to determine in situ forces of knee ligaments.* J Biomech, 1996. **29**(10): p. 1357-60.

72.A, M., C. C, R. A, L.P. Maletsky, and D. K. *Change in knee passive envelope of motion with total knee replacement design.* in *ASME Summer Bioengineering Conference*. 2008. Marco Island, Florida, USA.

73.Merican, A.M., E. Kondo, and A.A. Amis, *The effect on patellofemoral joint stability of selective cutting of lateral retinacular and capsular structures.* J Biomech, 2009. **42**(3): p. 291-6.

74.MacIntyre, N.J., N.A. Hill, R.A. Fellows, R.E. Ellis, and D.R. Wilson, *Patellofemoral joint kinematics in individuals with and without patellofemoral pain syndrome.* J Bone Joint Surg Am, 2006. **88**(12): p. 2596-605.

75.Zavatsky, A.B., P.T. Oppold, and A.J. Price, *Simultaneous in vitro measurement of patellofemoral kinematics and forces.* J Biomech Eng, 2004. **126**(3): p. 351-6.

76.Hashemi, J., N. Chandrashekar, T. Jang, F. Karpat, M. Oseto, and S. Ekwaro-Osire, *An Alternative Mechanism of Non-contact Anterior Cruciate Ligament Injury During Jump-landing: <i>In-vitro Simulation.* Experimental Mechanics, 2007. **47**(3): p. 347-354.

77.Bull, A.M., M.V. Katchburian, Y.F. Shih, and A.A. Amis, *Standardisation of the description of patellofemoral motion and comparison between different techniques.* Knee Surg Sports Traumatol Arthrosc, 2002. **10**(3): p. 184-93.

78..Farahmand, F., M.N. Tahmasbi, and A.A. Amis, *Lateral force-displacement behaviour of the human patella and its variation with knee flexion--a biomechanical study in vitro.* J Biomech, 1998. **31**(12): p. 1147-52.

79.Besier, T.F., C.E. Draper, G.E. Gold, G.S. Beaupre, and S.L. Delp, *Patellofemoral joint contact area increases with knee flexion and weight-bearing.* J Orthop Res, 2005. **23**(2): p. 345-50.

80.Salsich, G.B., S.R. Ward, M.R. Terk, and C.M. Powers, *In vivo assessment of patellofemoral joint contact area in individuals who are pain free.* Clin Orthop Relat Res, 2003(417): p. 277-84.

81.Chester, R., T.O. Smith, D. Sweeting, J. Dixon, S. Wood, and F. Song, *The relative timing of VMO and VL in the aetiology of anterior knee pain: a systematic review and meta-analysis.* BMC Musculoskelet Disord, 2008. **9**: p. 64.

82.Elias, J.J., S. Kilambi, D.R. Goerke, and A.J. Cosgarea, *Improving vastus medialis obliquus function reduces pressure applied to lateral patellofemoral cartilage.* J Orthop Res, 2009. **27**(5): p. 578-83.

83.Girgis, F.G., J.L. Marshall, and A. Monajem, *The cruciate ligaments of the knee joint. Anatomical, functional and experimental analysis.* Clin Orthop Relat Res, 1975(106): p. 216-31.

84.Hungerford, D.S. and M. Barry, *Biomechanics of the patellofemoral joint.* Clin Orthop Relat Res, 1979(144): p. 9-15.

85.Becher, C., R. Huber, H. Thermann, H.H. Paessler, and G. Skrbensky, *Effects of a contoured articular prosthetic device on tibiofemoral peak contact pressure: a biomechanical study.* Knee Surg Sports Traumatol Arthrosc, 2008. **16**(1): p. 56-63.

86. Miller, E.J., R.F. Riemer, T.L. Haut Donahue, and K.R. Kaufman, *Experimental validation of a tibiofemoral model for analyzing joint force distribution.* J Biomech, 2009. **42**(9): p. 1355-9.

87.Grood, E.S. and W.J. Suntay, *A joint coordinate system for the clinical description of three-dimensional motions: application to the knee.* J Biomech Eng, 1983. **105**(2): p. 136-44.

88. DeFrate, L.E., H. Sun, T.J. Gill, H.E. Rubash, and G. Li, *In vivo tibiofemoral contact analysis using 3D MRI-based knee models.* J Biomech, 2004. **37**(10): p. 1499-504.

89. Wretenberg, P., G. Nemeth, M. Lamontagne, and B. Lundin, *Passive knee muscle moment arms measured in vivo with MRI.* Clin Biomech (Bristol, Avon), 1996. **11**(8): p. 439-446.

90. Lo, J., O. Muller, M. Wunschel, S. Bauer, and N. Wulker, *Forces in anterior cruciate ligament during simulated weight-bearing flexion with anterior and internal rotational tibial load.* J Biomech, 2008. **41**(9): p. 1855-61.

91. Hartel, M.J., Y. Loosli, J. Gralla, S. Kohl, S. Hoppe, C. Roder, and S. Eggli, *The mean anatomical shape of the tibial plateau at the knee arthroplasty resection level: an investigation using MRI.* Knee, 2009. **16**(6): p. 452-7.

92. Gray, H., S. Standring, H. Ellis, and B.K.B. Berkovitz, *Gray's anatomy : the anatomical basis of clinical practice*. 39th ed2005, Edinburgh ; New York: Elsevier Churchill Livingstone. xx, 1627 p.

93. Johal, P., A. Williams, P. Wragg, D. Hunt, and W. Gedroyc, *Tibio-femoral movement in the living knee. A study of weight bearing and non-weight bearing knee kinematics using 'interventional' MRI.* J Biomech, 2005. **38**(2): p. 269-76.

94. Dennis, D.A., M.R. Mahfouz, R.D. Komistek, and W. Hoff, *In vivo determination of normal and anterior cruciate ligament-deficient knee kinematics.* J Biomech, 2005. **38**(2): p. 241-53.

# 7. Appendix

The appendix includes the patellofemoral kinematics for the eight cadaveric specimens before normalization. It also includes the medial and lateral lowest point and IE kinematics for the eight specimens used in chapter 4.

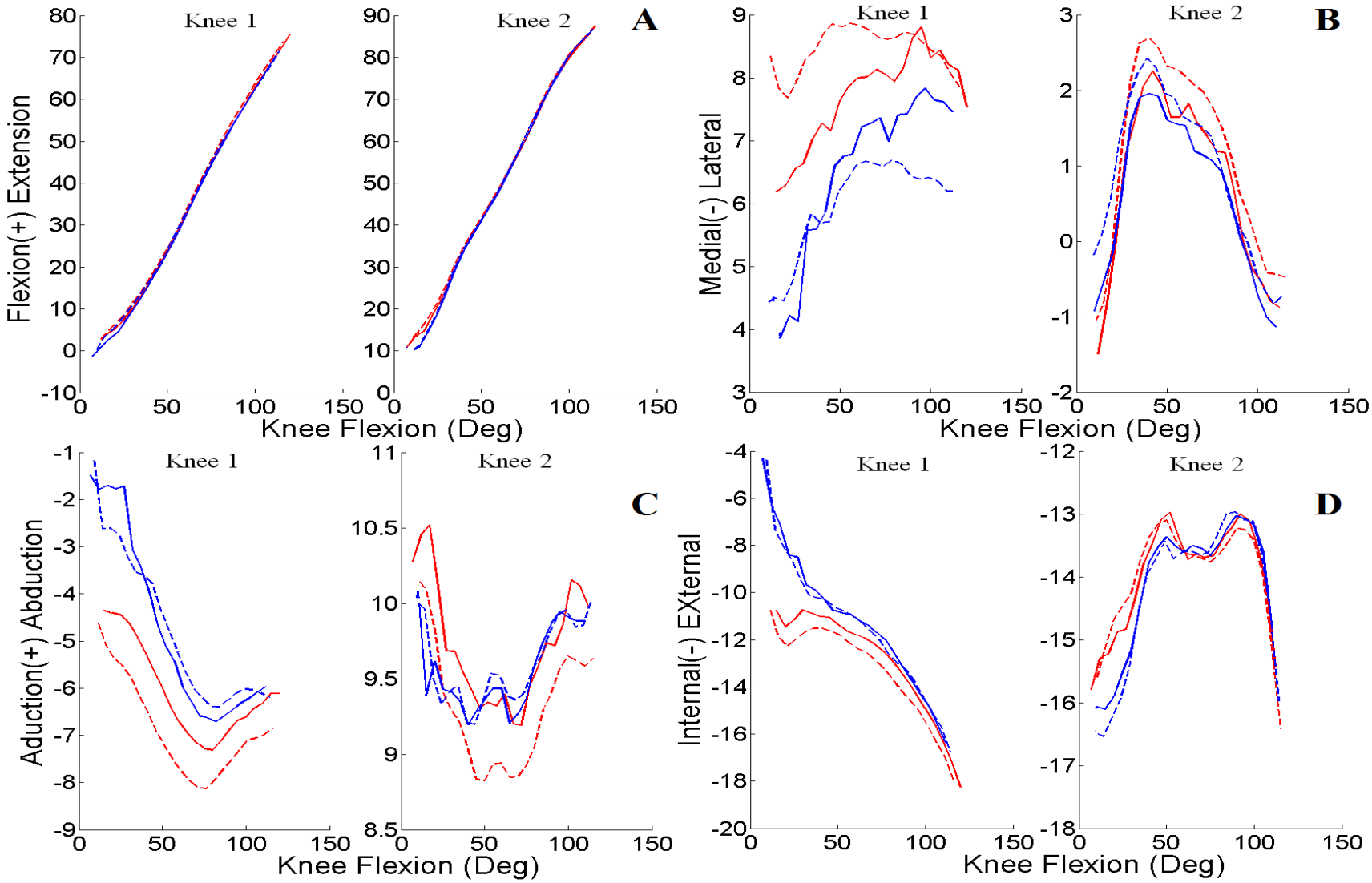


**Figure 7.1: the four patellar tracking measures for the two knee that receive both Ma and Mo protocols A) flexion, B) shift, C) tilt, and D) rotation SMa (solid blue), SMo (dashed blue), NMa (solid red), and NMo ( dashed red).**

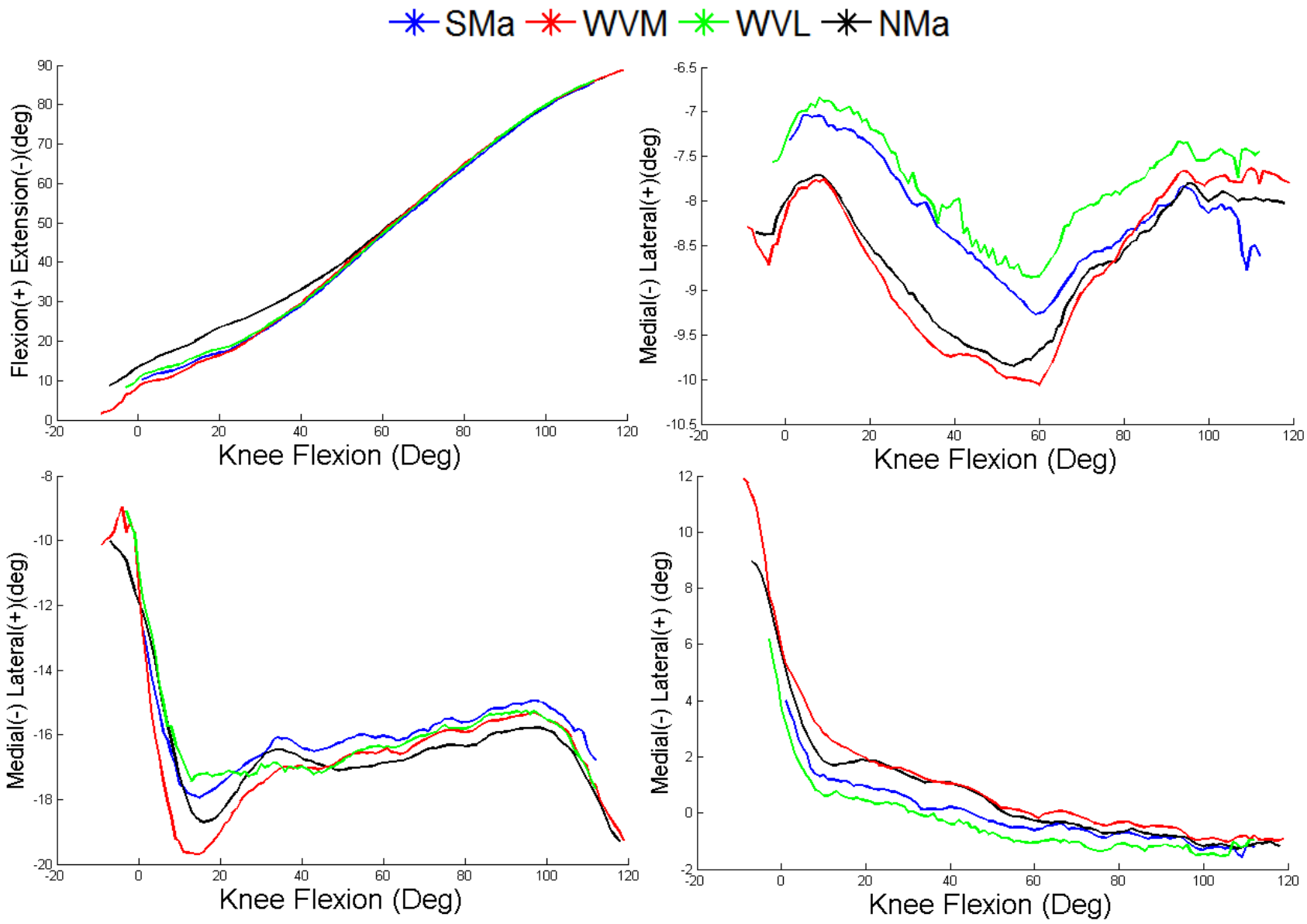


**Figure 7.2: The four patellar tracking measures of knee 1: A) flexion, B) shift, C) tilt, and D) rotation for the SMa (Blue), WVM (Red), WVL (green), and NMa (black) in the three-axis orthogonal coordinate system before normalization.**

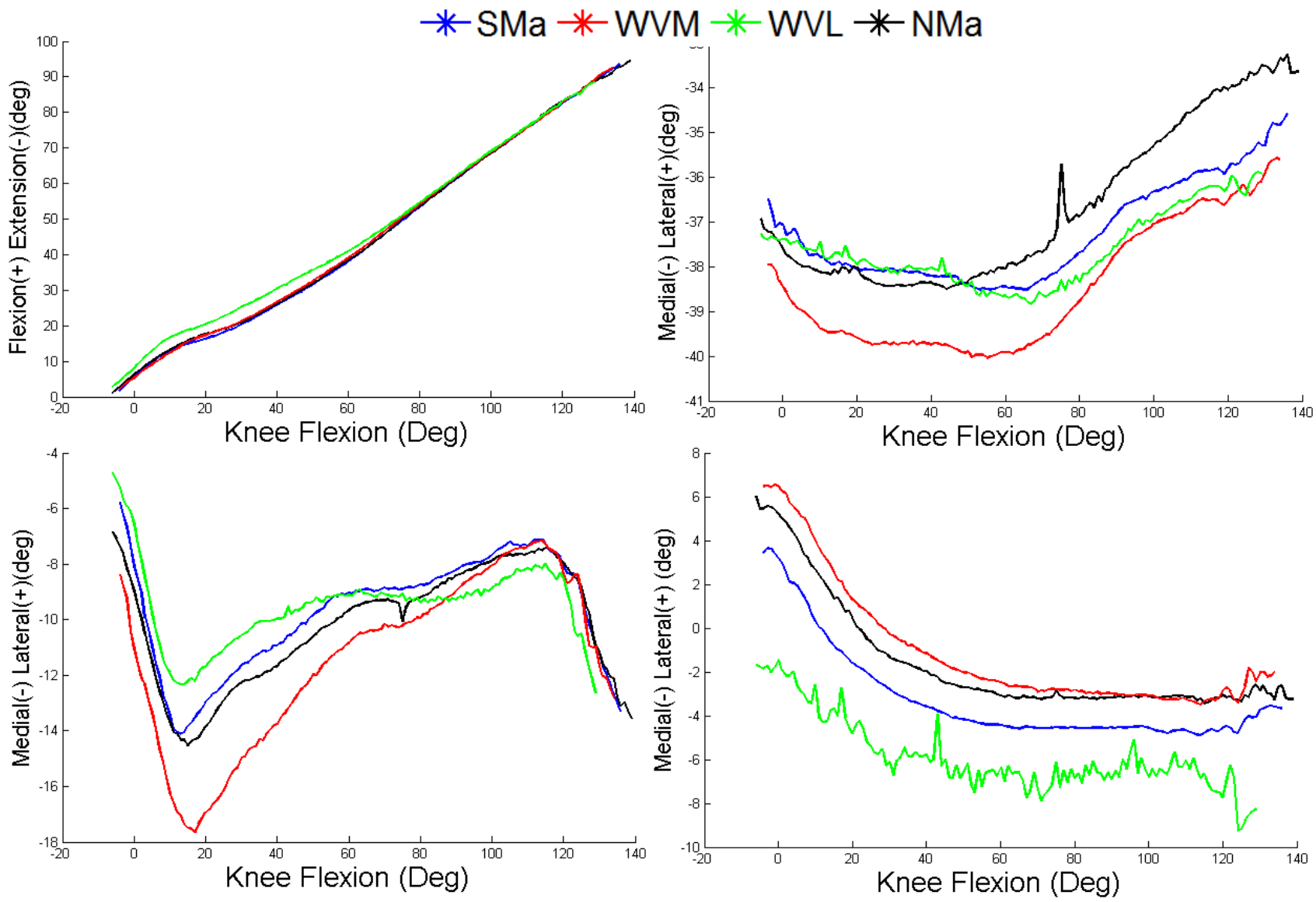


**Figure 7.3: The four patellar tracking measures of knee 2: A) flexion, B) shift, C) tilt, and D) rotation for the SMa (Blue), WVM (Red), WVL (green), and NMa (black) in the three-axis orthogonal coordinate system before normalization.**

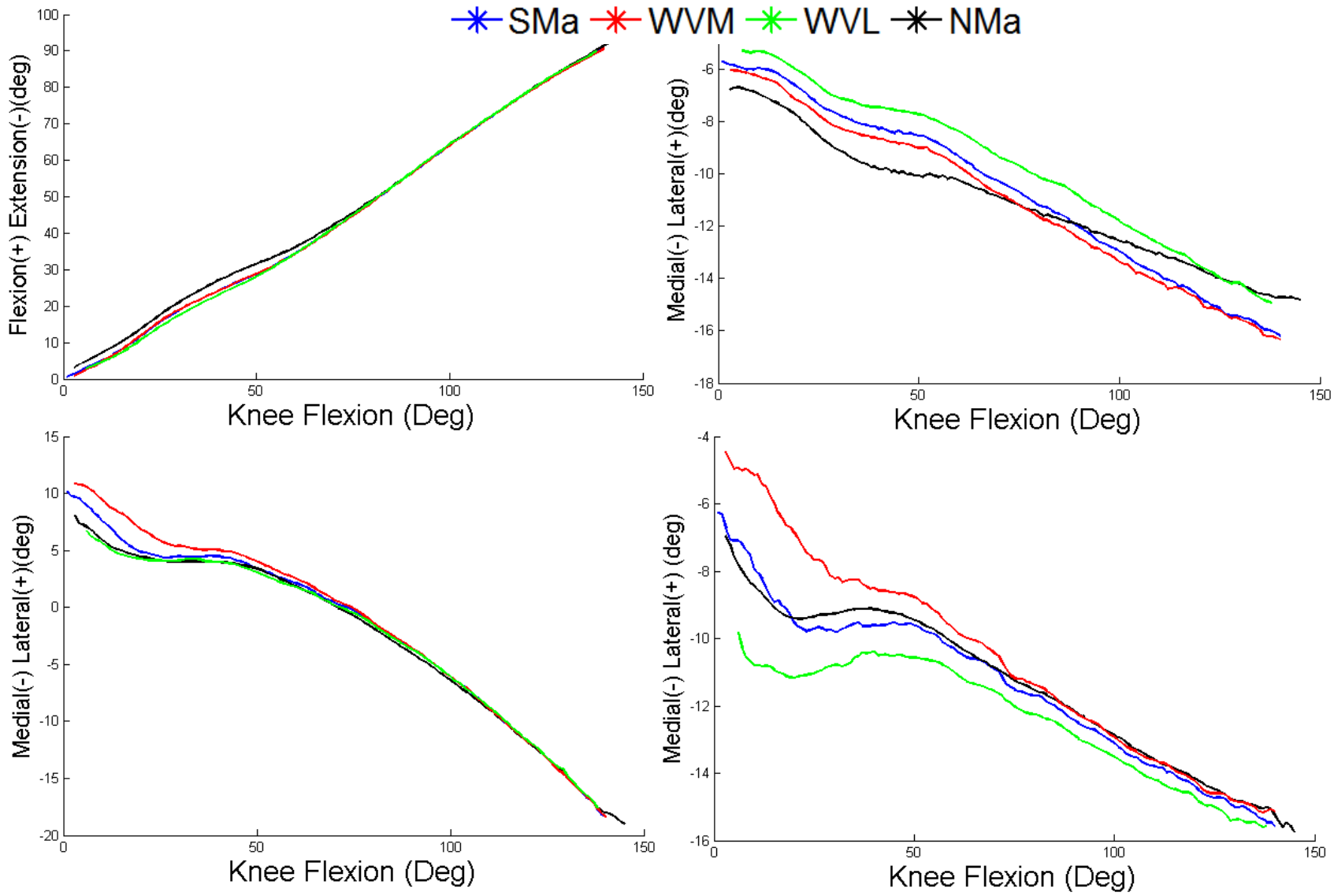


**Figure 7.4: The four patellar tracking measures of knee 3: A) flexion, B) shift, C) tilt, and D) rotation for the SMa (Blue), WVM (Red), WVL (green), and NMa (black) in the three-axis orthogonal coordinate system before normalization.**

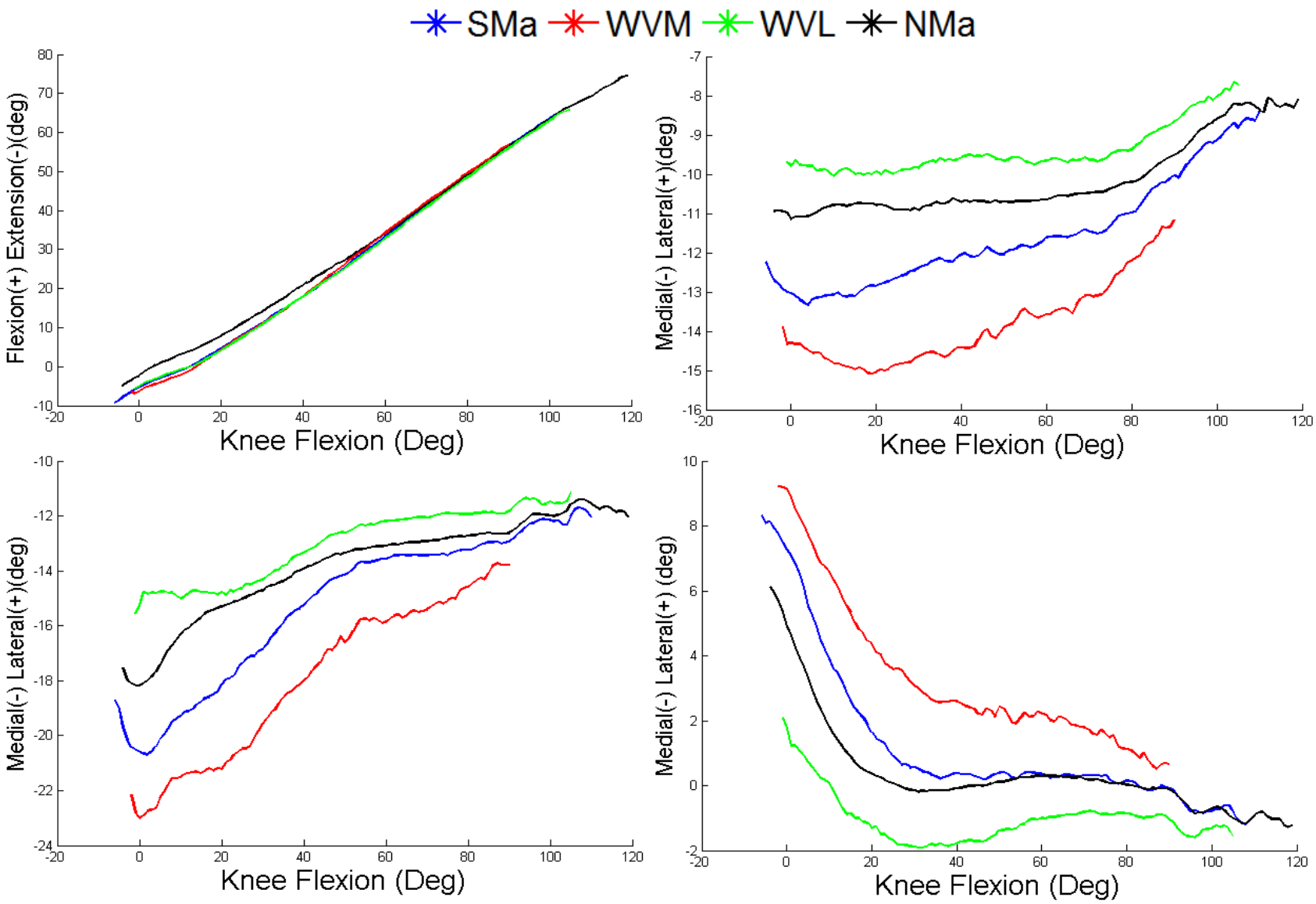


**Figure 7.5: The four patellar tracking measures of knee 4: A) flexion, B) shift, C) tilt, and D) rotation for the SMa (Blue), WVM (Red), WVL (green), and NMa (black) in the three-axis orthogonal coordinate system before normalization.**

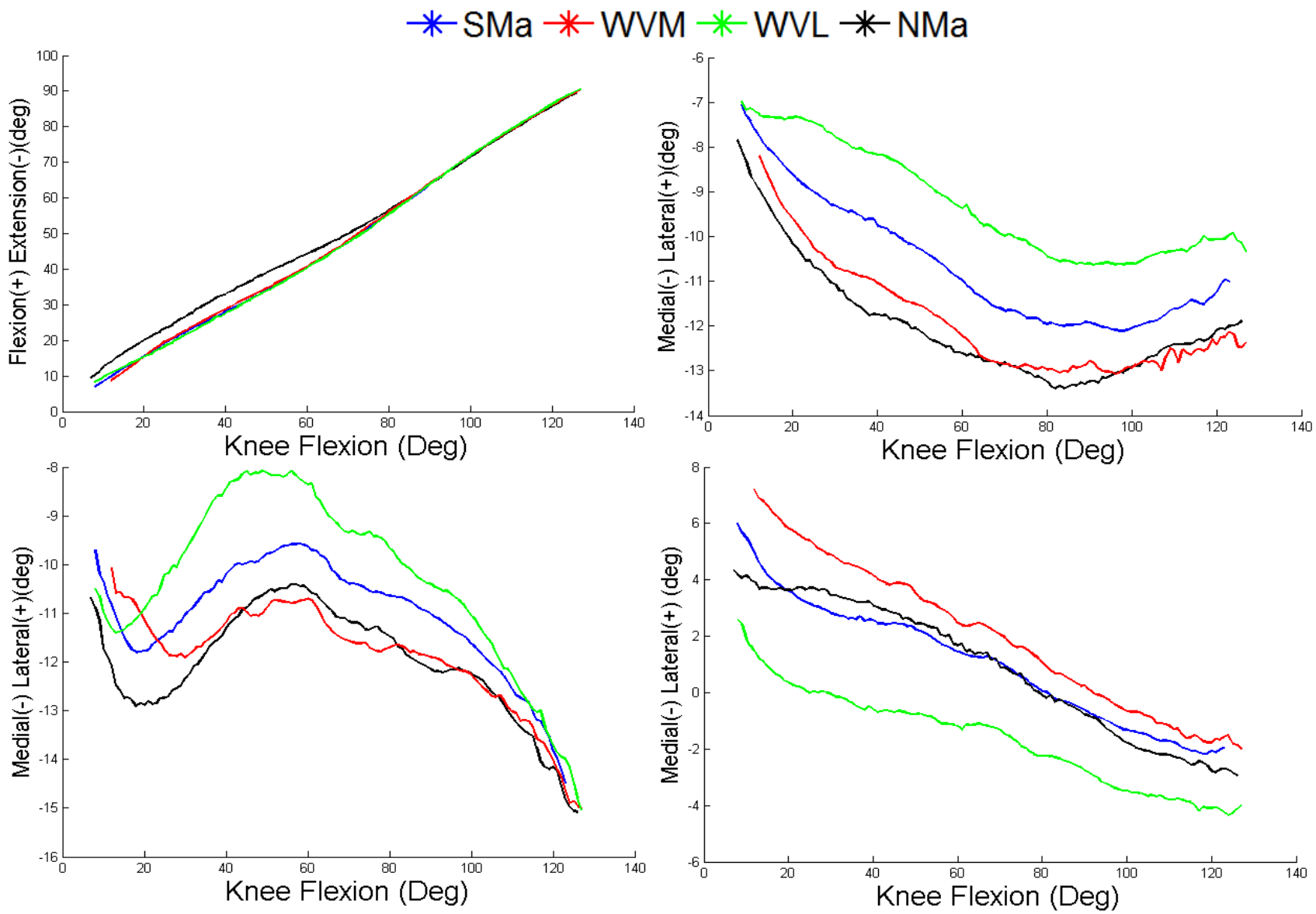


**Figure 7.6: The four patellar tracking measures of knee 5: A) flexion, B) shift, C) tilt, and D) rotation for the SMa (Blue), WVM (Red), WVL (green), and NMa (black) in the three-axis orthogonal coordinate system before normalization.**

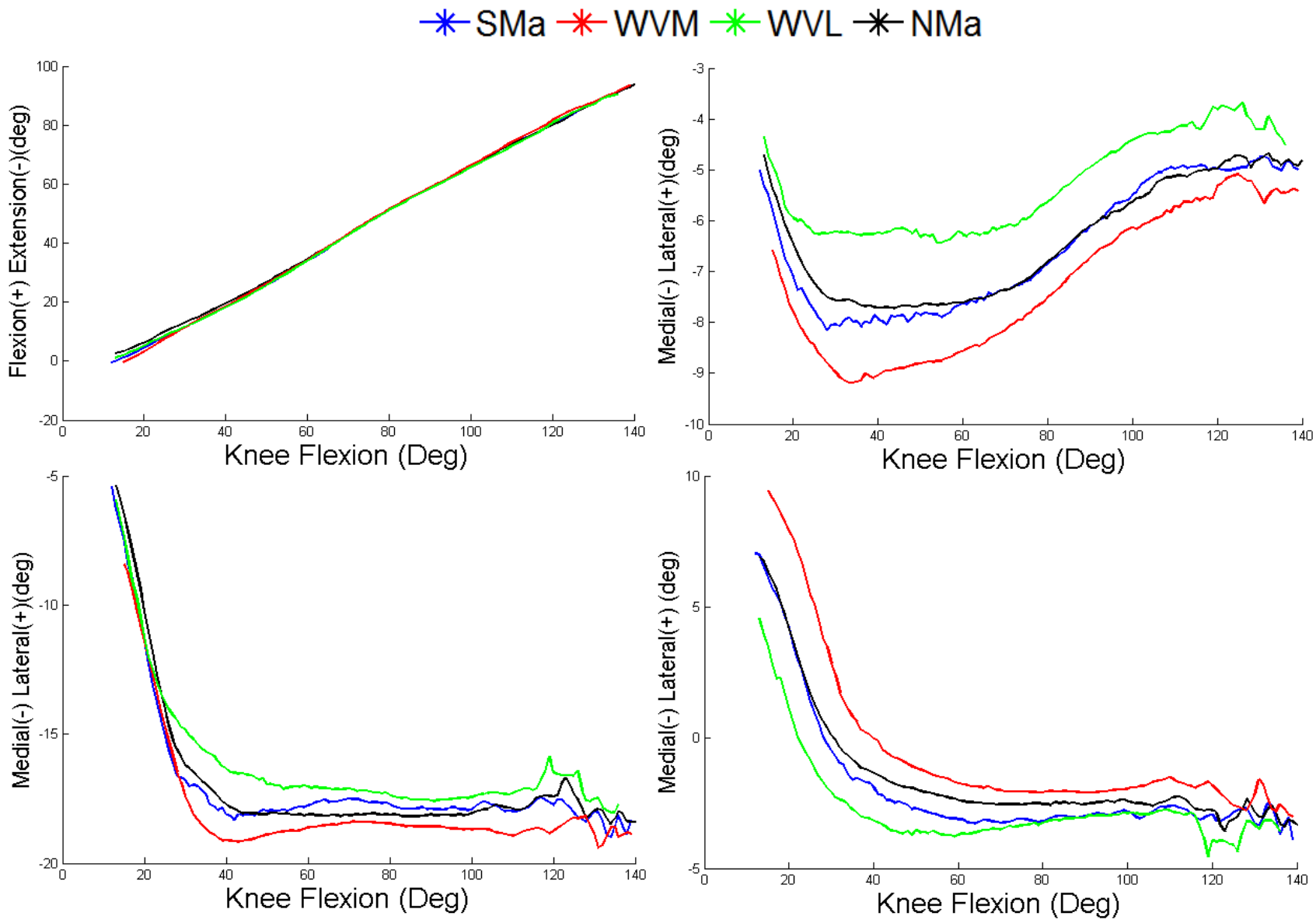


**Figure 7.7: The four patellar tracking measures of knee 6: A) flexion, B) shift, C) tilt, and D) rotation for the SMa (Blue), WVM (Red), WVL (green), and NMa (black) in the three-axis orthogonal coordinate system before normalization.**

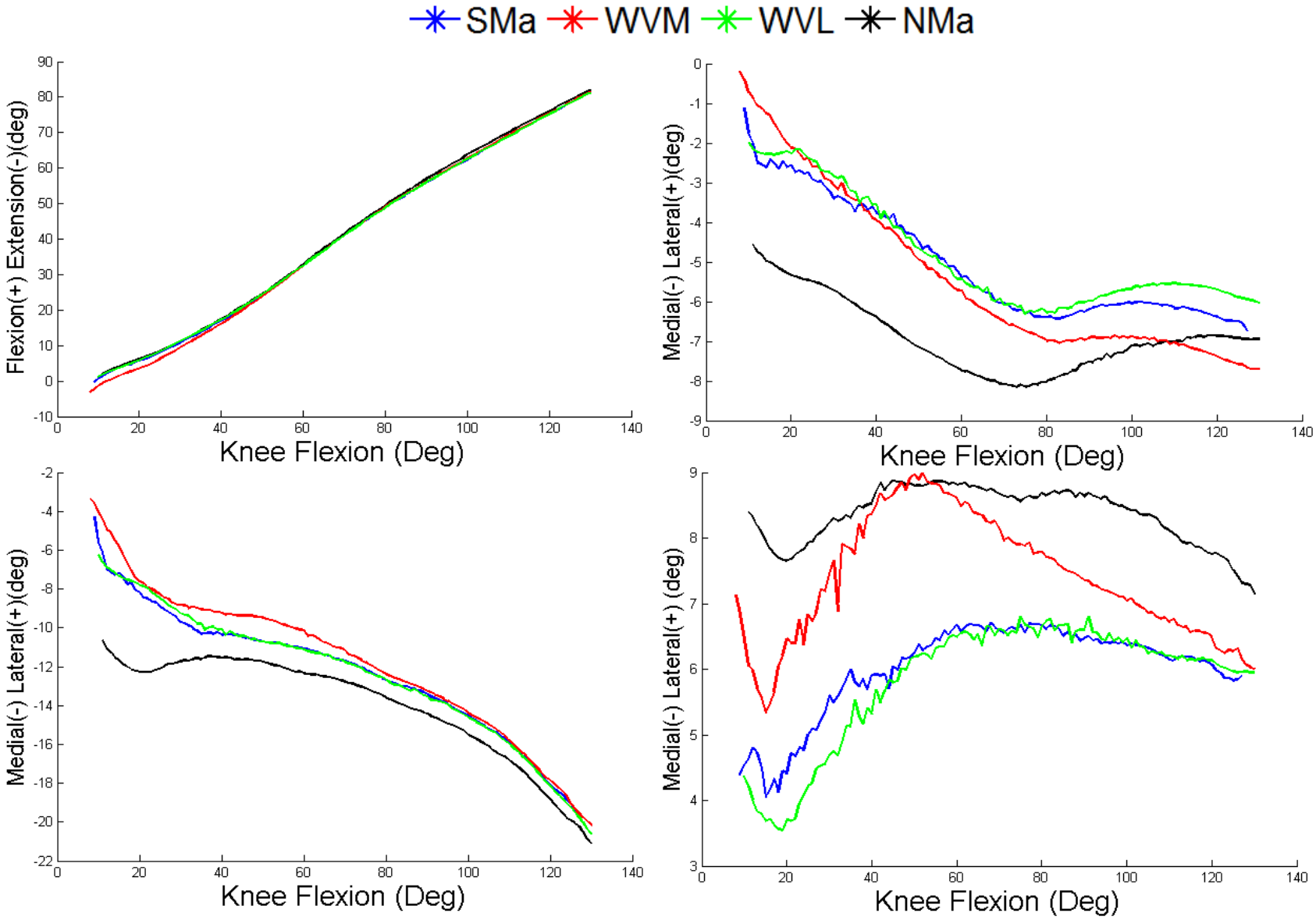


**Figure 7.8: The four patellar tracking measures of knee 7: A) flexion, B) shift, C) tilt, and D) rotation for the SMa (Blue), WVM (Red), WVL (green), and NMa (black) in the three-axis orthogonal coordinate system before normalization.**

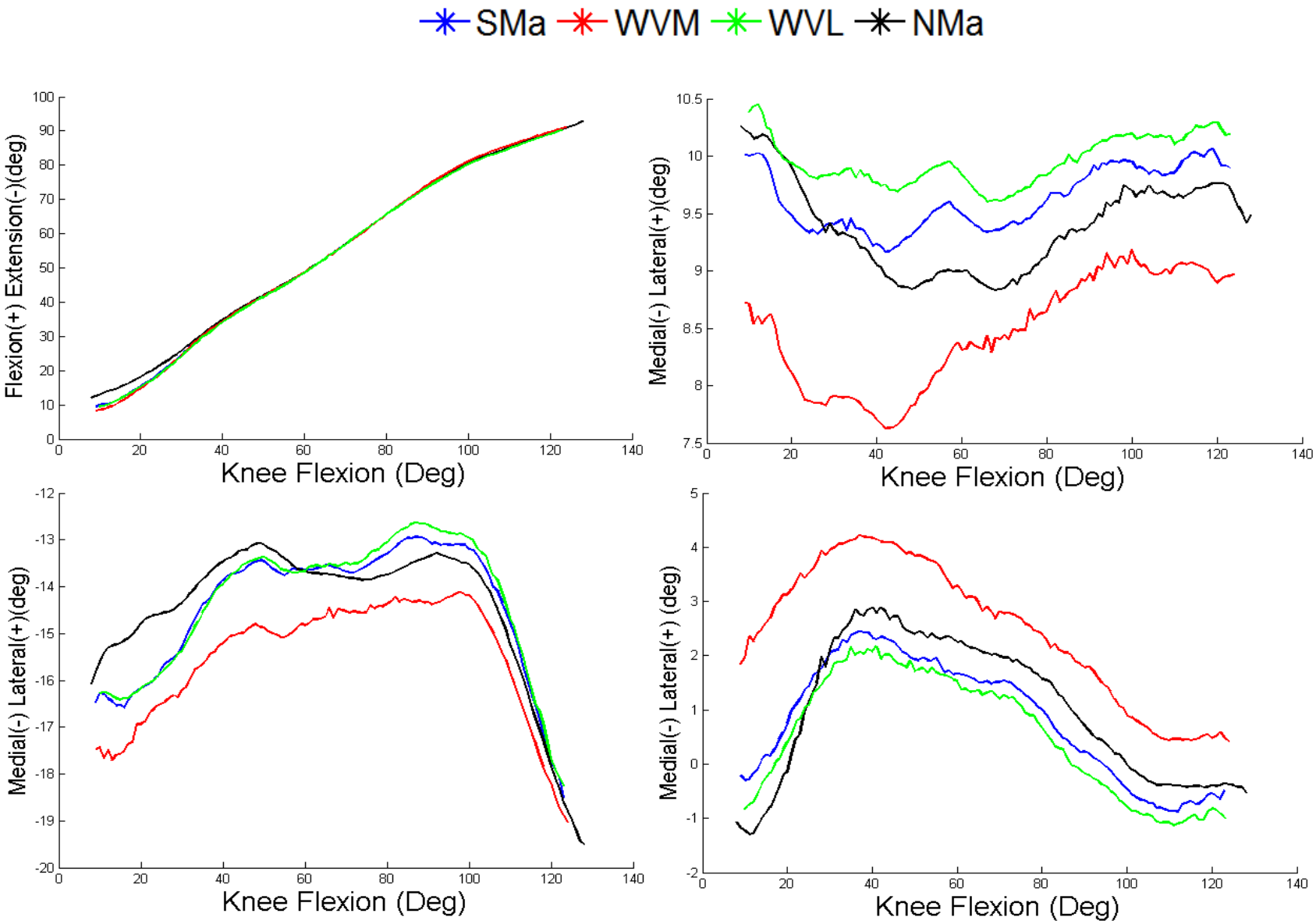


**Figure 7.9: The four patellar tracking measures of knee 8: A) flexion, B) shift, C) tilt, and D) rotation for the SMa (Blue), WVM (Red), WVL (green), and NMa (black) in the three-axis orthogonal coordinate system before normalization.**

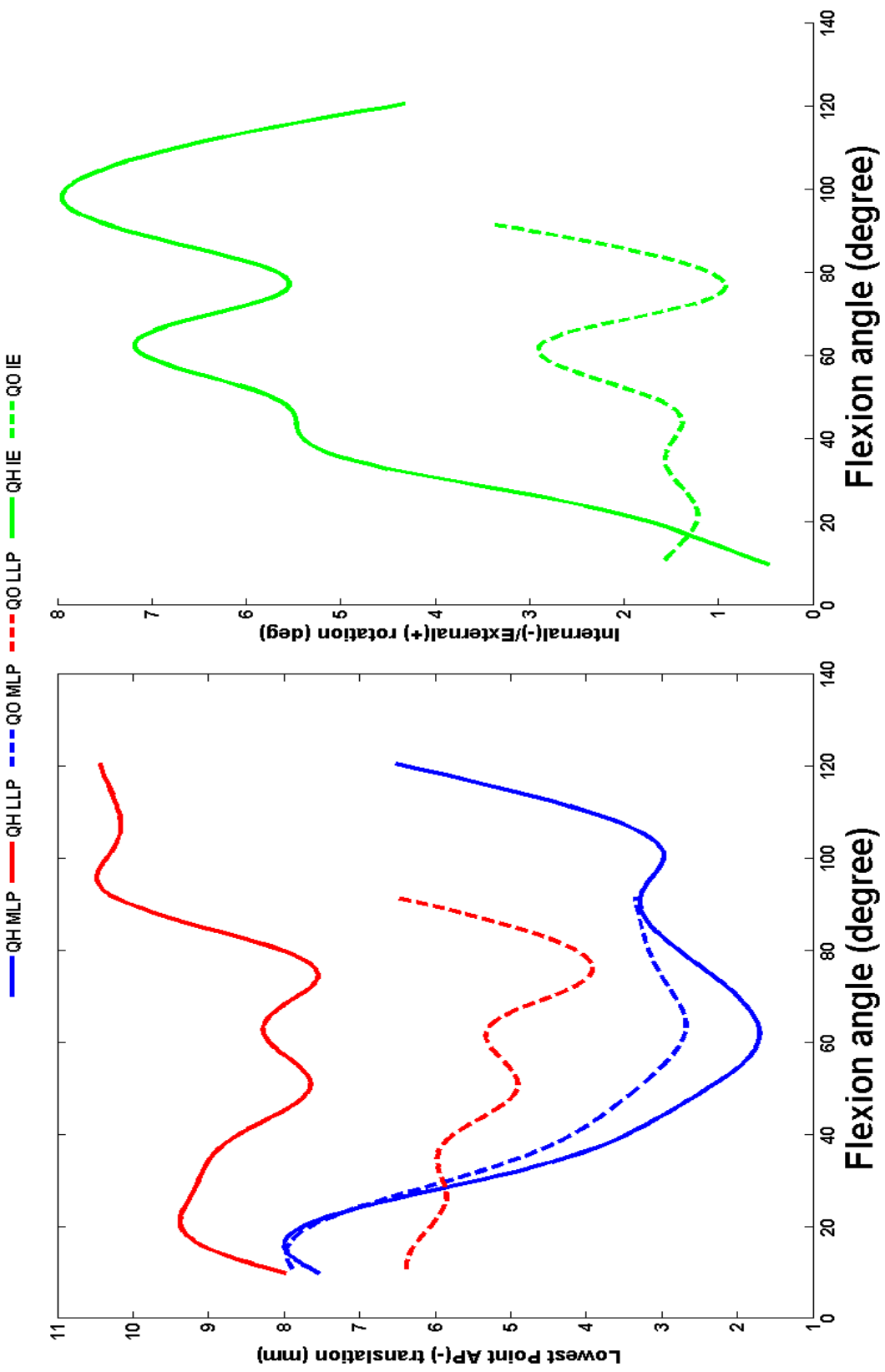


**Figure 7.10: knee 1's medial (red) and lateral (blue) lowest point (left) and IE (right) kinematics for both QH (solid) and QO (dashed) configuration.**

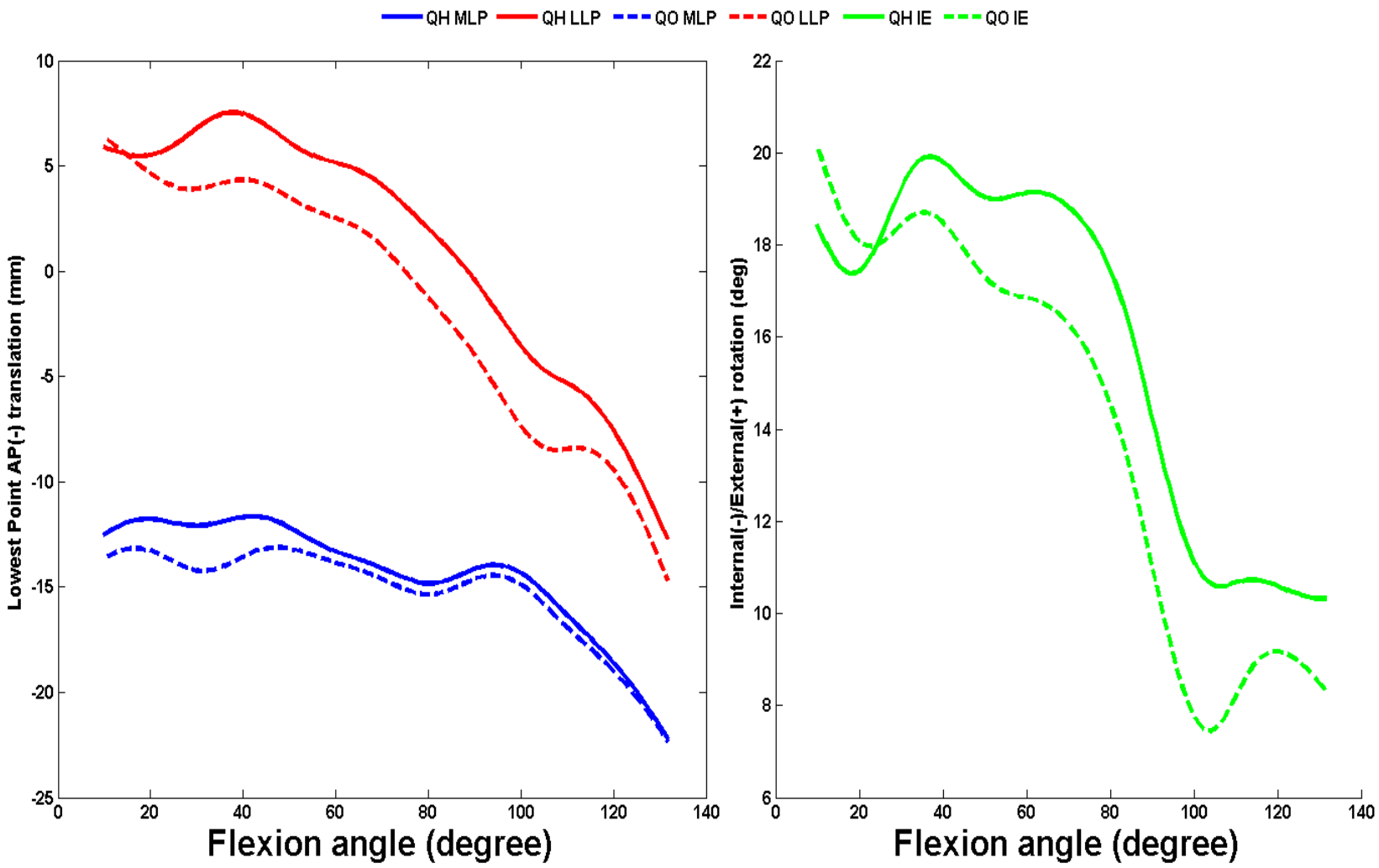


**Figure 7.11: knee 2's medial (red) and lateral (blue) lowest point (left) and IE (right) kinematics for both QH (solid) and QO (dashed) configuration.**

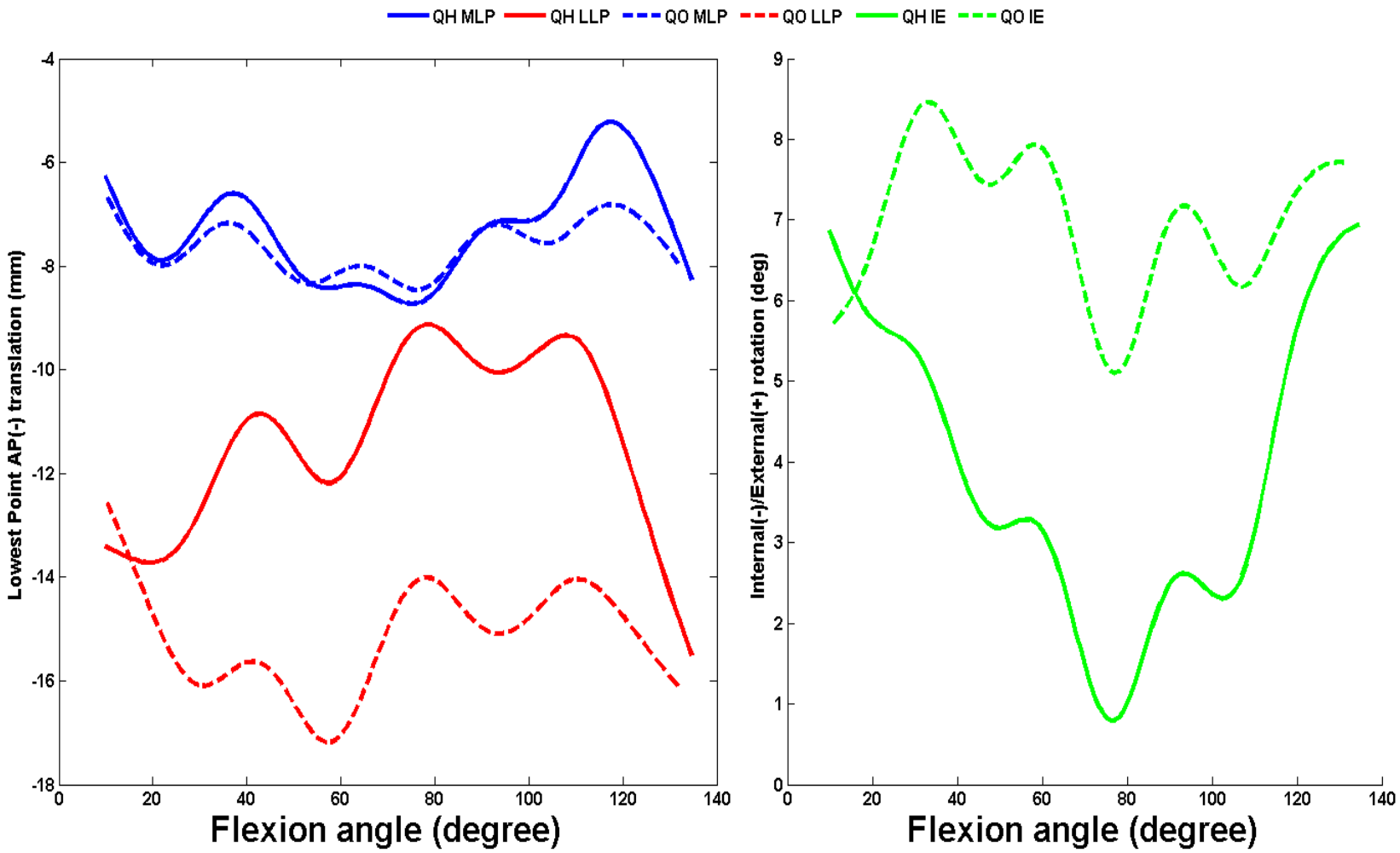


**Figure 7.12: knee 3's medial (red) and lateral (blue) lowest point (left) and IE (right) kinematics for both QH (solid) and QO (dashed) configuration.**

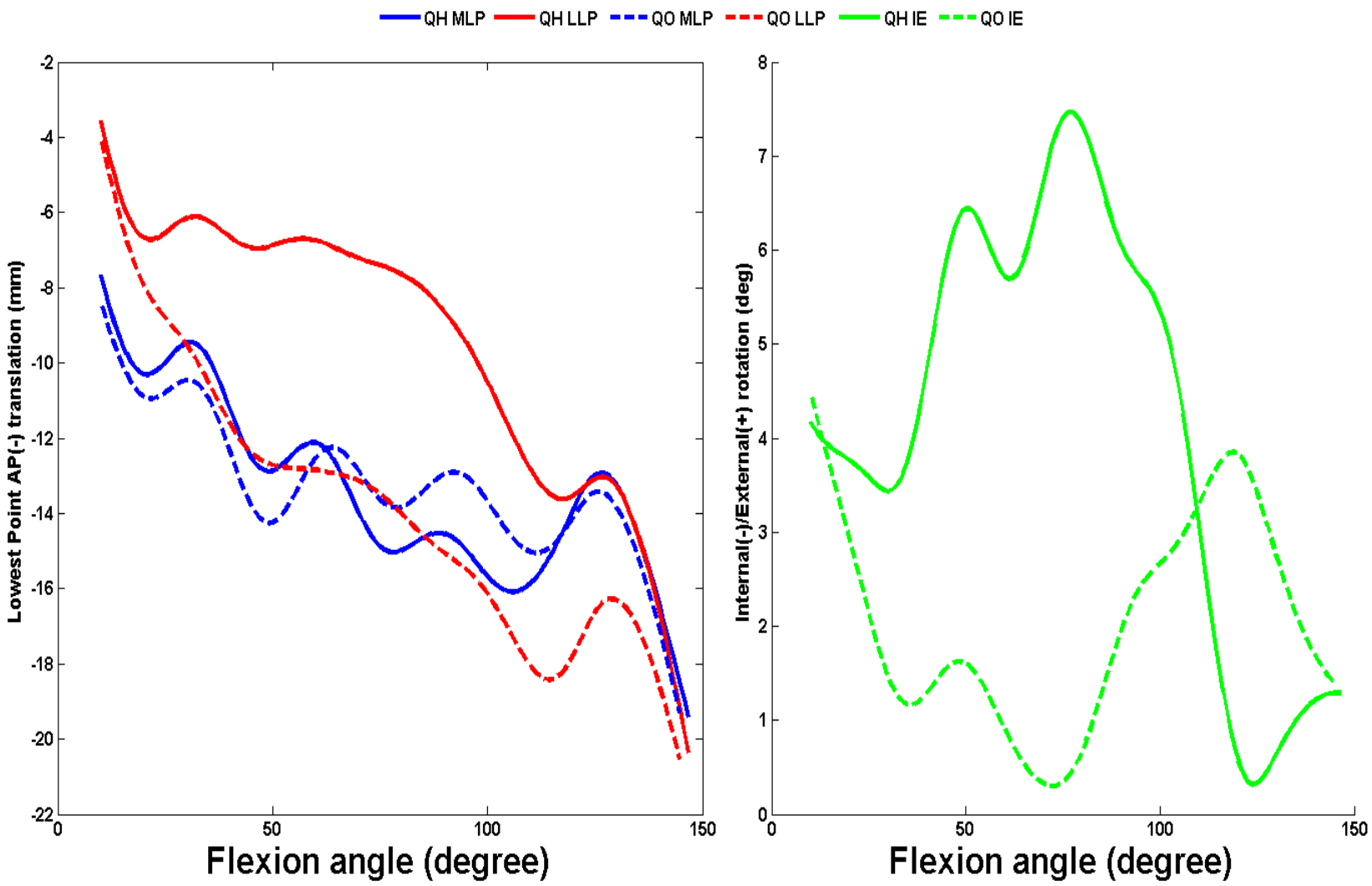


**Figure 7.13: knee 4's medial (red) and lateral (blue) lowest point (left) and IE (right) kinematics for both QH (solid) and QO (dashed) configuration.**

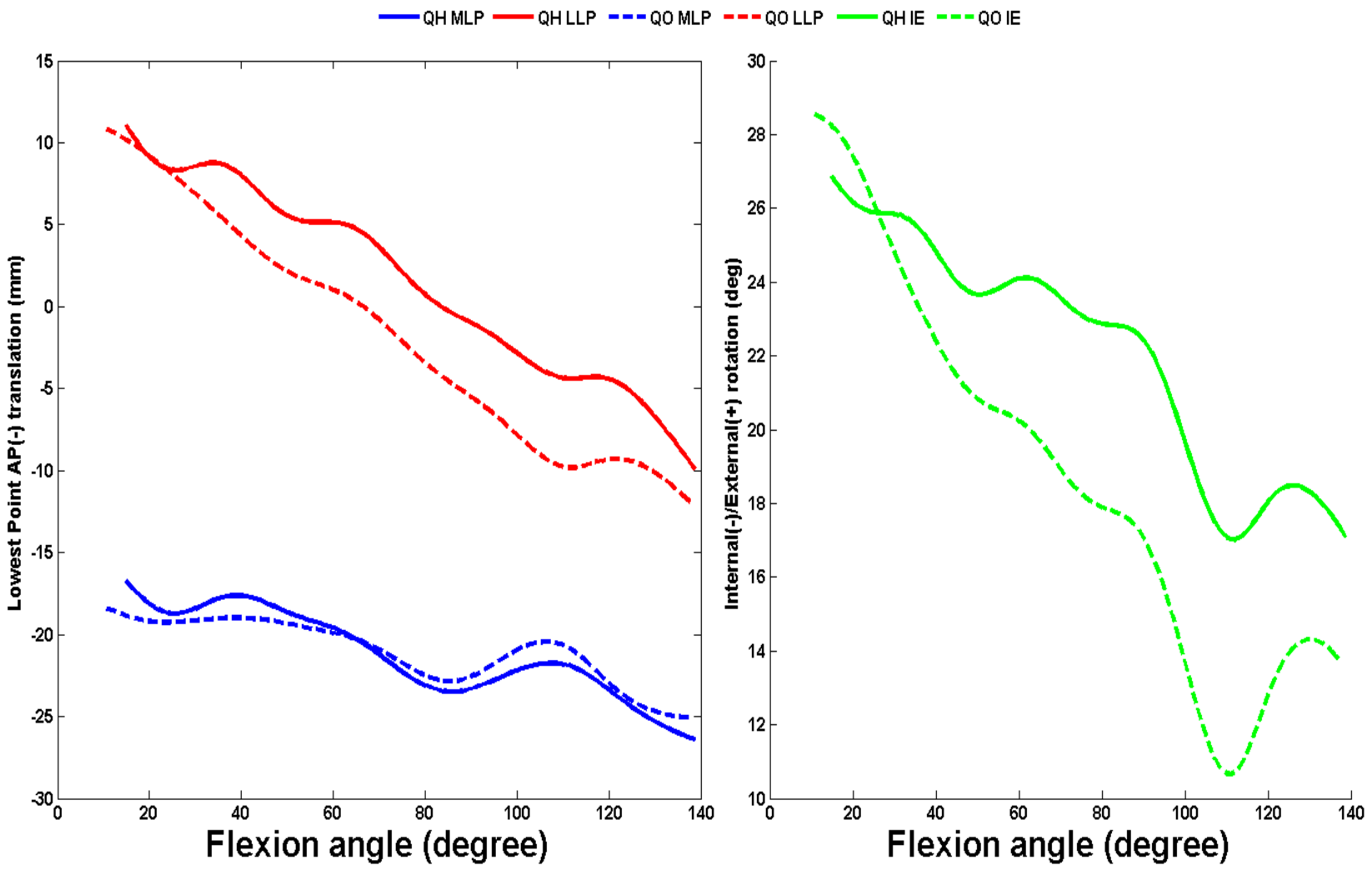


**Figure 7.14: knee 5's medial (red) and lateral (blue) lowest point (left) and IE (right) kinematics for both QH (solid) and QO (dashed) configuration.**

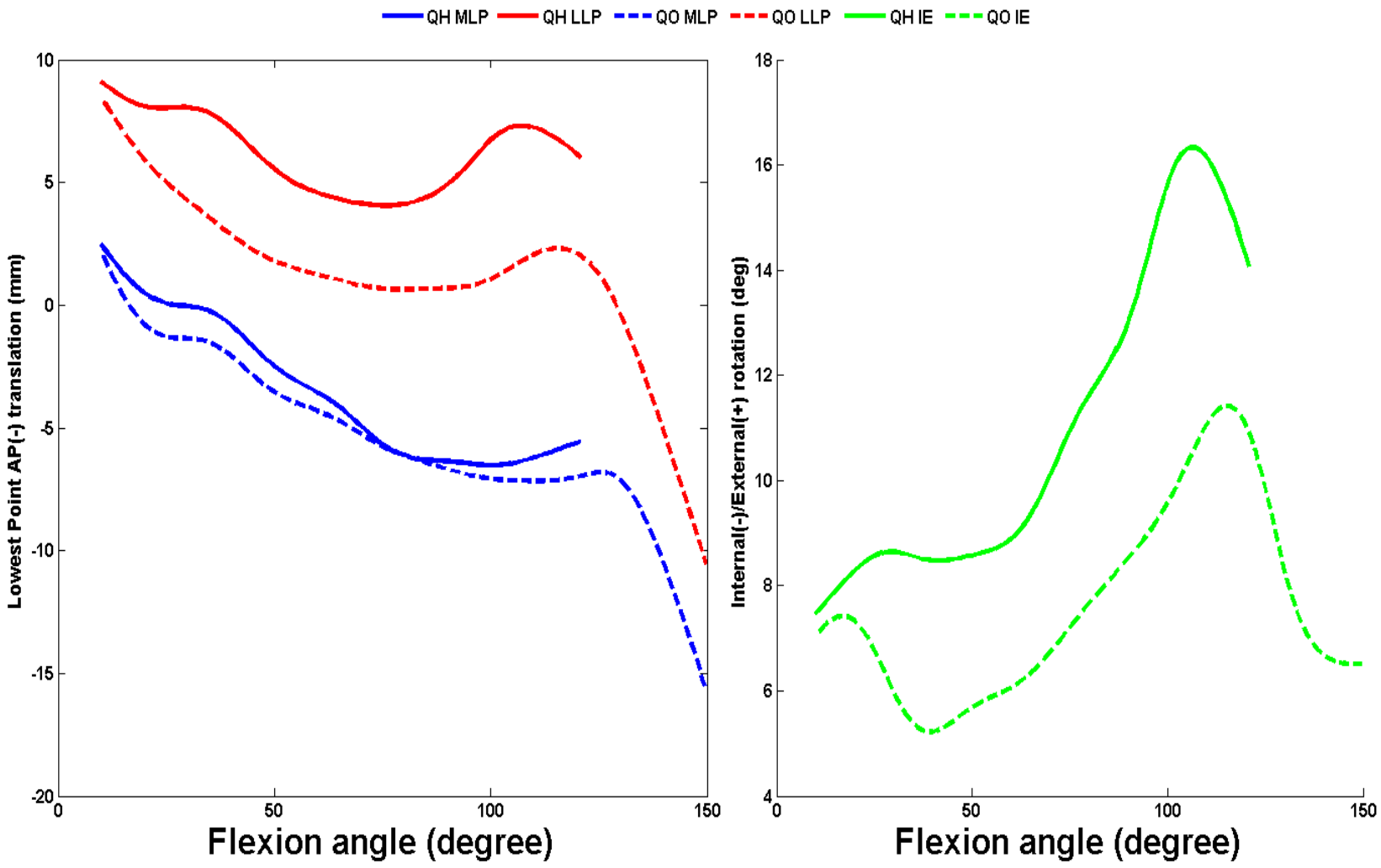


**Figure 7.15: knee 6's medial (red) and lateral (blue) lowest point (left) and IE (right) kinematics for both QH (solid) and QO (dashed) configuration.**

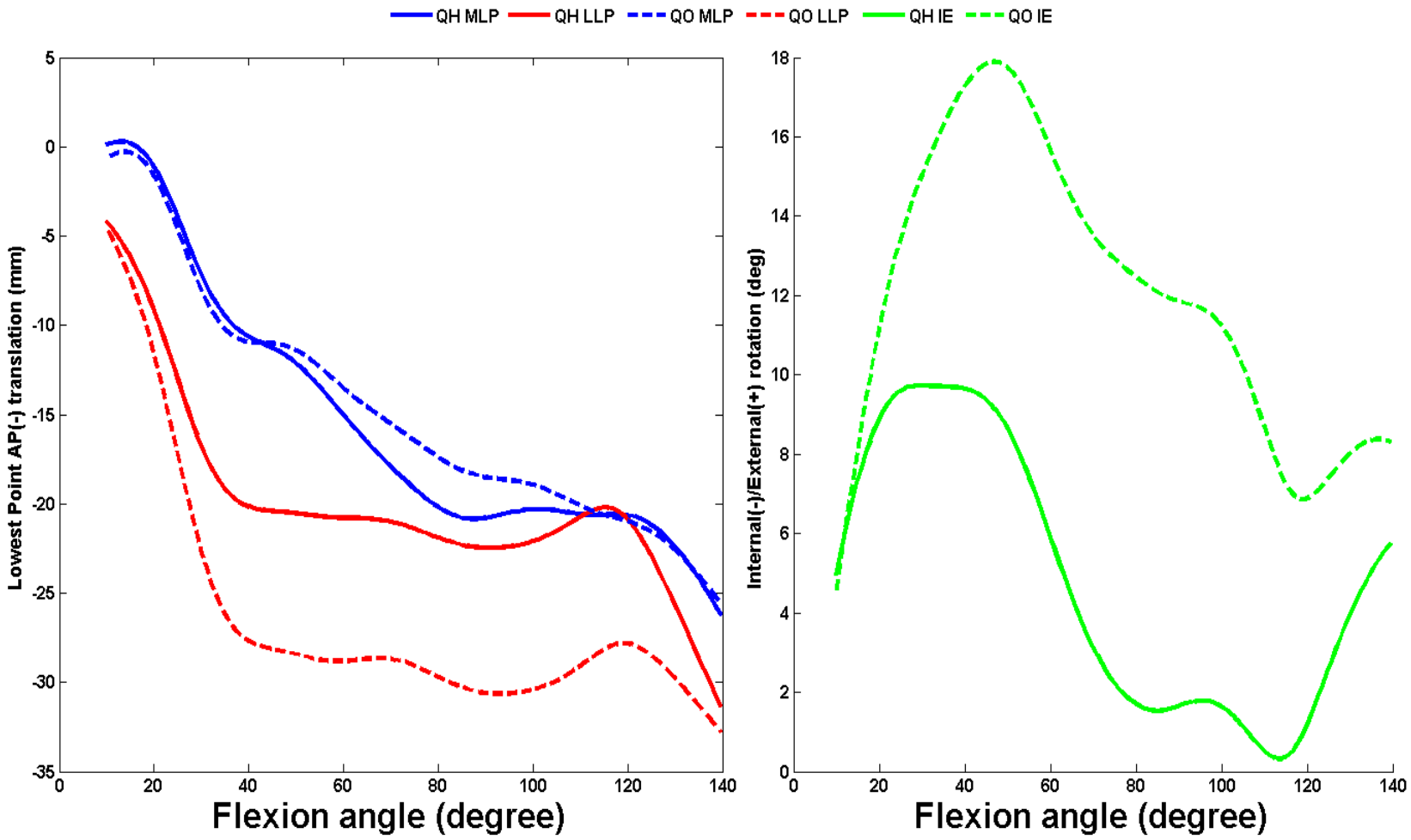


**Figure 7.16: knee 7's medial (red) and lateral (blue) lowest point (left) and IE (right) kinematics for both QH (solid) and QO (dashed) configuration.**

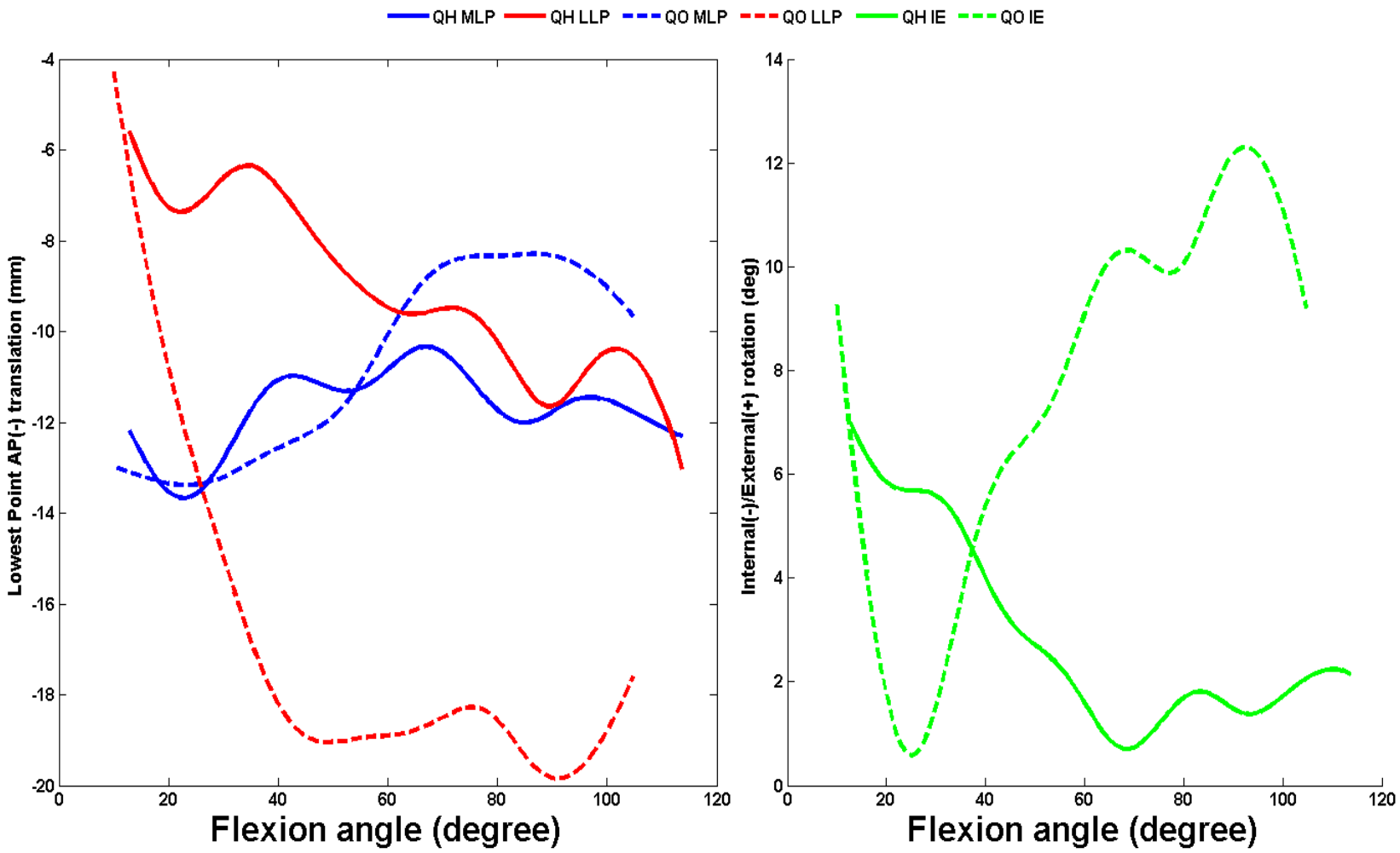


**Figure 7.17: knee 8's medial (red) and lateral (blue) lowest point (left) and IE (right) kinematics for both QH (solid) and QO (dashed) configuration.**